BPJ 410

FINAL REPORT

AN OPERATIONS RESEARCH AND SIMULATION-BASED STUDY ON IMPROVING THE EFFICIENCY OF A SLURRY DRYING TOWER

by

EBEN DE JONGH

28092547

Acknowledgements

I would like to thank the following people who made a contribution to both the project and my ability to complete it.

Jozine Botha, my mentor, for her patience in advising me and always being willing to go the extra mile.
Professor Yadavalli, the Head of Department whose door was always open to provide technical operational research insight.
My parents for their ongoing support and confidence in my academic ability.
The Unilever engineering and human resource departments, particularly Orvando Ferreira and Jade Badenhorst for unselfishly giving of their time.
My Heavenly Father for providing me with the ability and perseverance to complete the undertaking.

Executive Summary

Safe-guarding the environment is one of, if not the most, important contemporary issues faced by society today. This project deals with this issue, and relates to the Unilever washing powders factory in Boksburg. The focus is on improving the efficiency of gas usage (per unit of powder produced) in the furnace that produces hot air. This hot air is an integral part of washing powder production: it dries the viscous slurry and transforms it into the base powder used in all washing powders. The cost of gas is the factory's largest expense, and – considering that for every 1GJ of gas burned, 55.8kg of CO_2 is produced – it is a pollutant too. Improving furnace efficiency is thus of utmost importance in the successful operation of the factory and in reducing its impact on the environment.

Lances are nozzles that spray slurry into the drying tower; the spraying slurry forms a conical shape, represented by circles in a cross-sectional view. There are two layers of lances in the drying tower: 24 in the top layer and 18 in the bottom layer. Currently, individual operators select which lances should run, based on the required output; thus no standard operating procedure is followed. This leads to substantial variation in the coverage of slurry within the tower, as there are four shifts per day. Ultimately, the efficiency of operations is negatively impacted, and more gas is burnt. In this project, the configuration and positioning of these lances is investigated, and an optimal solution is found by using an operations research approach to the solution of the circle packing problem (CPP). The solution to the CPP is used to find the positioning of the top layer of lances. The positions of the bottom layer of lances are determined by filling the largest open spaces within the tower. These positions are found using geometry and trigonometry. The final proposed configuration of lances balances the amount of slurry overlap and open spaces within the tower to provide the optimal solution. By finding this balance, gas usage is reduced and energy is saved.

To solve the above-mentioned problems, an operations research model of the process is built using MATLAB and the non-linear optimiser called SNOPT (Sparse Non-Linear Optimiser), and the optimal solution is found. SNOPT is a MATLAB add-on that specifically addresses non-linear optimisation problems, and is produced by TOMLAB. A Microsoft Excel simulation of the slurry coverage within the tower is used to show the cross-sectional coverage of slurry originating from each lance within the tower. The operations research model optimises the coverage of slurry of the top layer of lances. This model serves to optimise and standardise the lance positioning within the tower, thus increasing the productivity and profitability of the operations.

Contents

Acknowledgements ... i

Executive Summary ... ii

List of Figures ... vi

List of Tables ... viii

List of Algorithms ... ix

List of Acronyms ... x

Chapter 1 ... 1

Introduction and Background ... 1

1.1 Unilever ... 1

1.2 Project Introduction ... 1

1.3 Problem Statement ... 2

1.4 Benefit to Unilever ... 4

1.5 Project Aim ... 6

1.6 Project Scope ... 6

1.7 Deliverables ... 7

1.8 Project Plan ... 7

1.8.1 Activities and Tasks ... 7

Chapter 2 ... 8

Literature Review ... 8

2.1 Problem Identification ... 8

2.2 Introduction to the Circle Packing Problem ... 8

2.3 Lance Assignment Problem ... 9

2.3.1 Heuristic Algorithm of Birgin and Sorbal ... 9

2.3.2 Monotonic and Population Basin Hopping ... 10

2.3.3 Energy Landscaping Paving (ELP) ... 10

2.3.4 Formulation Space Search ... 10

2.3.5 TomSym Modelling ... 13

2.3.6 Packomania Website ... 14

2.4 Excel Simulation of Lance Positioning ... 14

2.5 Change Management 15
Chapter 3 17
Solution Approach 17
3. 1 Attribute Identification 17
3.1.2 Classification of Overlap 21
3.1.3 Classification of Open Spaces 23
3.2 Solution Explanation 24
Chapter 4 27
Model Execution and Comparison 27
4.1 Operations Research Solution 27
4.2 Analysis of Current Configuration 28
4.2.1 Overlap Analysis 29
4.2.2 Open Space Analysis 39
4.3 Analysis of Proposed Configuration 42
4.3.1 Overlap Analysis 43
4.3.2 Open Space Analysis 43
4.4 Configuration Comparison 44
4.5 Results Validation 47
Chapter 5 49
Conclusion 49
5.1 Recommendations for Implementation 49
5.2 Conclusion 49
References 50
Appendix A 52
Factory Information 52
Appendix B 53
Current oscillation of gas usage 53
Appendix C 54
Current configuration and lance numbering 54

Appendix D ... 57
Calculation of Bottom Lance Layer Positions ... 57
Description of Second Layer Lance Positioning ... 59
Appendix E ... 61
Calculation of overlapping circles ... 61
Appendix F ... 66
Converting the solution from a unit circle container to the appropriate nine metre diameter .. 66
Appendix G ... 68
MATLAB coding: Formulation Space Search ... 68
Appendix H ... 75
MATLAB coding: TomSym ... 75
Appendix I ... 77
Coordinates of solution ... 77
Appendix J ... 79
Proposed Lance Order of Opening ... 79

List of Figures

Figure 1: Graphical representation of Level One lance positioning with accompanying slurry coverage ... 3
Figure 2: Graphical representation of Level Two lance positioning with accompanying slurry coverage ... 3
Figure 3: Graphical representation of combined lance positioning and slurry coverage ... 4
Figure 4: Illustration of overlap resulting in distorted slurry flow ... 5
Figure 5: Graphical illustration of SMART change ... 15
Figure 6: Illustration of coordinate system used ... 18
Figure 7: Photographic representation of lance nozzle spraying slurry at an angle of 61° ... 18
Figure 8: Graphical representation of lance nozzle spraying slurry at an angle of 61° ... 19
Figure 9: Graphical illustration of tapering of slurry fall ... 20
Figure 10: Illustration of nozzle angle changes ... 20
Figure 11: Graphical representation of nozzle angle and the resulting distortion of the cross-sectional view of the cone ... 21
Figure 12: Graphical representation of an example of first degree overlap ... 23
Figure 13: Graphical representation of an example of second degree overlap ... 23
Figure 14: Graphical representation of an example of third degree overlap ... 23
Figure 15: Graphical representation of effect of increasing the scale of solution ... 25
Figure 16: Revised current lance configuration, so that it is circular ... 29
Figure 17: Illustration of FDO calculation ... 31
Figure 18: Reducing the effect of free spaces resulting in TDO ... 34
Figure 19: Pie chart illustrating proportions of differing areas of overlap ... 36
Figure 20: Histogram illustrating occurrences of overlap per classification ... 37
Figure 21: Histogram illustrating the instances of overlap per classification ... 37
Figure 22: Illustration of slurry originating from the bottom layer of lances making contact with the tower ... 38
Figure 23: Graphical representation of open spaces in current configuration of lances ... 39
Figure 24: Effect of eliminating a TDS ... 40
Figure 25: Pie chart illustrating the occurrences of open space classifications ... 41
Figure 26: Pie chart illustrating the occurrences of FDS and SDS only ... 41
Figure 27: Proposed configuration to be analysed ... 42
Figure 28: Diagrammatic representation of open spaces in proposed configuration of lances .. 44
Figure 29: Comparison of top lance layer positioning of current and proposed configurations . 45
Figure 30: Comparison of bottom lance layer positioning of current and proposed configuration ... 46
Figure 31: Comparison of lance positioning and slurry coverage of currrent and proposed configuration ... 47

Figure 32: Basic factory layout, Unilever Boksburg 52
Figure 33: Oscillation of gas usage.. 53
Figure 34: Illustration of top layer lance positioning and numbering with accompanying slurry coverage for current configuration 54
Figure 35: Illustration of bottom layer lance positioning and numbering with accompanying slurry coverage for current configuration 55
Figure 36: Illustration of top and bottom layer lance positioning with accompanying slurry coverage for current configuration 56
Figure 37: Illustration of lance numbering for the top layer of the proposed solution 57
Figure 38: Illustration of final lance positioning with accompanying slurry flow......................... 58
Figure 39: Overlapping circles calculation demonstration circles.. 61
Figure 40: Calculation of diameter of circle.. 64

List of Tables

Table 1: Illustration of overlap duplication avoidance 31
Table 2: Table showing occurrence and area (m^2) of FDO 32
Table 3: Table showing occurrences and area (m^2) of SDO 33
Table 4: Table showing occurrence and area (m^2) of TDO 35
Table 5: Overlap statistics per classification 38
Table 6: Table showing all occurrences of overlap within the proposed configuration 43
Table 7: Cartesian coordinates of cross-sectional slurry flow of current lance positioning 62
Table 8: Reduced table of distances between circle centres 63
Table 9: Reduced table of distances between overlapping circles 64
Table 10: Further modified table of distances between circle centres 65
Table 11: Reduced table of overlapping areas between circles 65
Table 12: The Cartesian coordinates and radii of contained circles within a unit circle container 66
Table 13: Table showing the Cartesian coordinates and radii of contained circles within a 4.5m radius circular container 67

List of Algorithms

Algorithm 1: Formulation Space Search pseudo-code..13

Algorithm 2: TomSym Solution pseudo-code..15

List of Acronyms

CPP	**C**ircle **P**acking **P**roblem
FDO	**F**irst **D**egree **O**verlap
FDS	**F**irst **D**egree **S**paces
FSS	**F**ormulation **S**pace **S**earch
MATLAB	**MAT**rix **LAB**oratory
NP	**N**ondeterministic **P**olynomial time
PMC	**P**owder **M**oisture **C**ontent
SCA	**S**lurry **C**one **A**ngle
SDO	**S**econd **D**egree **O**verlap
SDS	**S**econd **D**egree **S**paces
SMART	**S**pecific **M**easurable **A**ctionable **R**ealistic **T**ime-bound
SMC	**S**lurry **M**oisture **C**ontent
SNOPT	**S**parse **N**onlinear **OPT**imiser
TDO	**T**hird **D**egree **O**verlap
TDS	**T**hird **D**egree **S**paces

Chapter 1

Introduction and Background

1.1 Unilever

Unilever is a multi-national, multi-product corporation with over 400 brands being produced and sold in Europe, Asia, Africa, the Middle East, and the Americas. Unilever has a strong presence in the South African washing detergent sector, owning brands such as Sunlight, Omo, Skip, and Surf. All of these powders are produced in their Boksburg factory, which is where this project has been carried out.

1.2 Project Introduction

To produce washing powder, slurry (high viscosity liquid) is produced by mixing a combination of solids and liquids. The slurry is then transported through two pumps: first a low pressure pump and then a high pressure one. A diagrammatic representation of the factory can be seen in Appendix A. This slurry is then sprayed, at a high pressure of approximately 50 bars, into a drying tower through what is called a lance. There are 42 lances in the tower: 24 in the top layer and 18 in the bottom layer. In the tower, below the lances, are 18 vents symmetrically positioned to extract the hot air from the furnace into the drying tower. Thus, as the hot air rises and the slurry falls, a phase change takes place as the moisture from the slurry evaporates. In the process the slurry becomes powder. The powder falls on to a conveyor belt and the powder moisture content (PMC) is measured. This base powder is then altered by adding components in specified ratios, according to the product being made. (For example, Skip, OMO, and Surf all have exactly the same base powder. Differentiation occurs by adding different components.) The finished product is then packaged on-site, stacked on to palettes, and transported all over South Africa.

The focus of the project is on improving the functioning and efficiency of the furnace and the drying tower. Each lance has the capacity to spray 1.67 tons of slurry per hour. After the slurry has been de-moisturised, the powder weighs around 30% less than the slurry, depending on the moisture content. The inlet temperature of the air entering the tower varies according to the amount of gas burned, as well as the amount and temperature of air pumped into the furnace. This temperature varies from 300 to 450 °C. An important indicator of the efficiency of the tower is the top temperature in relation to the inlet temperature and PMC. The higher the top temperature, the less efficiently the tower is working. This means that the hot air is not evaporating the moisture; instead the air rises through the gaps in the slurry and heats the top of the tower.

1.3 Problem Statement

The problem in question relates to the configuration and positioning of the lances spraying slurry into the drying tower. Figures 1 to 3 illustrate the coverage of the spraying slurry at one-and-a-half metres below the lance. The containing circle represents the circumference of the drying tower. The blue and red circles represent the cross-sectional area of the slurry being sprayed from the top and bottom layers of lances respectively. One notices that much overlap occurs between the blue and red circles. Overlapping slurry leads to variation in the density of slurry falling within the tower, which ultimately causes the uneven drying of powder.

When examining Figures 1, 2, and 3 below, one also notices a substantial amount of free space in slurry coverage. These open spaces allow heat (and therefore energy) to 'escape' without directly drying the slurry; and this leads to inefficiency. This inefficiency will be clearly signified and noticed when one examines the relationship between the inlet temperature and the top temperature. The key influence on this relationship is the amount of free space in the tower. The laws of physics tell us that energy will always move through the path with least resistance. This principle is easily explained and understood when examining electric current and resistors. If there is a current of 100 amperes and two resistors A and B (in parallel) with 5Ω and 10 Ω respectively, twice as much of the current will pass through A than through B. The same principle applies to the gaps in the falling slurry: more super-heated gas will rise through the openings between the slurry than through the falling slurry itself.

When optimising the spraying lance configuration, the optimal solution is one where slurry coverage within the tower is maximised. By maximising the surface area of the falling slurry, gas consumption will be reduced. As a direct result, Unilever will save money and reduce its carbon footprint. This widespread inefficiency, caused by a sub-optimal configuration of the lances within the tower, is regarded as the problem to be solved.

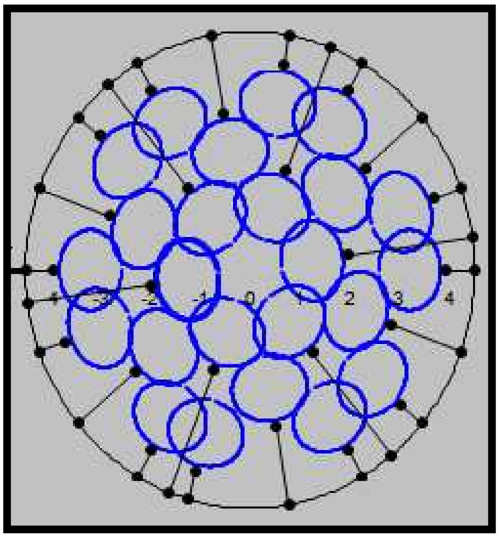

Figure 1: Graphical representation of Level One lance positioning with accompanying slurry coverage

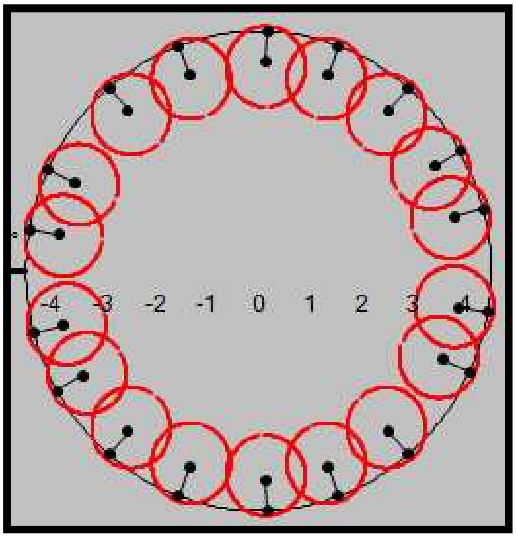

Figure 2: Graphical representation of Level Two lance positioning with accompanying slurry coverage

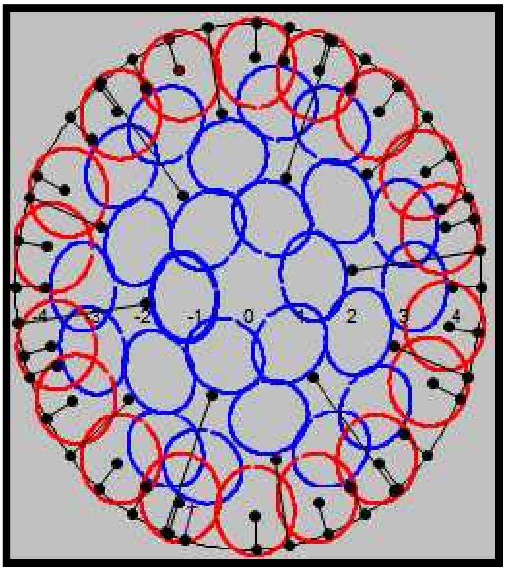

Figure 3: Graphical representation of combined lance positioning and slurry coverage

1.4 Benefit to Unilever

When proposing the implementation of a project, it is of the utmost importance to stress the potential benefit to the organisation. This notion is particularly pertinent at Unilever, given the competitive corporate landscape in which it operates. Every opportunity to improve processes and operations significantly should be explored, and – when viable – the opportunity should be implemented.

If the lance configuration problem is sufficiently solved, Unilever can expect the following benefits:

- ***Decreased overlap of slurry within tower***

The drying ability of the slurry is inversely related to the slurry density, which is affected by slurry overlap within the tower. When the slurry overlap within the tower decreases, it dries more evenly and efficiently, leading to better powder quality by improving the consistency of the PMC. As overlap occurs, the density of slurry within the overlapping space radically increases, and this impairs its drying ability. The more the overlap occurs, the more uneven and disrupted the flow and density of the slurry will become. This trend is illustrated in Figure 4 below. If overlap within the tower is minimised, the slurry density will remain more constant. This will have positive implications for the powder quality, and in particular the powder moisture content (PMC).

The PMC is regulated through a feedback loop. The PMC is measured on a conveyor as it falls out of the drying tower. If the powder is too dry, less air and gas is used by the furnace;

conversely, more air and gas will be used if the PMC is too high. This causes oscillations in the use of air and gas. These changes are illustrated by the graphs found in Appendix C.

Ultimately, if the solution decreases overlap within the tower, Unilever will experience a decrease in the consumption, and more even usage, of natural gas within the furnace. Gas is Unilever Powders' biggest expense in producing washing powder, so the implementation of a successful solution should be considered.

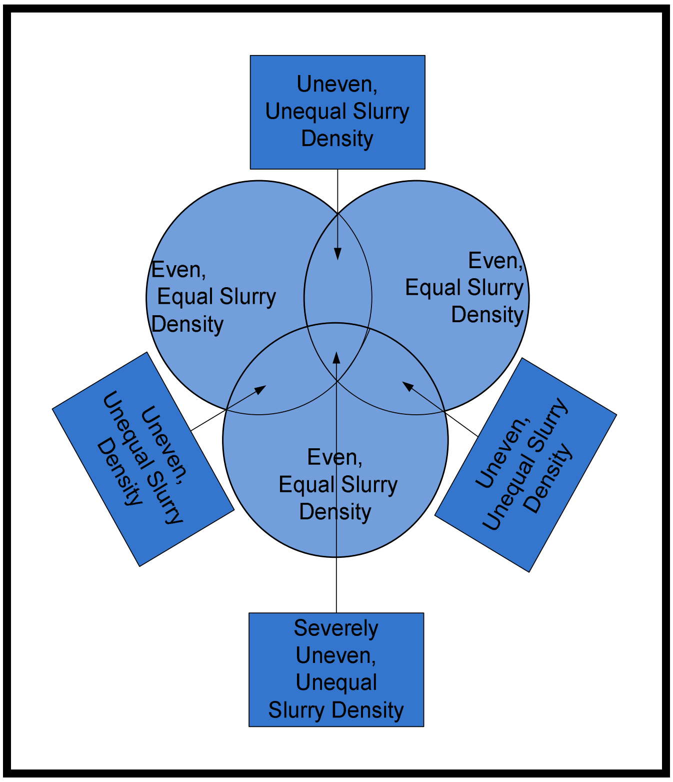

Figure 4: Illustration of overlap resulting in distorted slurry flow

- ***Decreased size and number of gaps in slurry***

Gaps in the slurry within the drying tower create areas of 'no resistance'. As the slurry falls and the hot air rises, the hot air passes through these areas of least resistance. When this happens, the energy used to heat the air by burning gas is wasted – because the energy will heat the top of the tower instead of directly drying the slurry.

The size and number of gaps can be increased by changing the positioning of the lances within the tower, thus saving an immense amount of gas. The factory is run almost continually, day and night, almost all year round. Thus, a small hourly saving on gas will quickly become substantial when the tower is running 150 hours a week.

- **Operational uniformity**

Currently there is a large amount of variation within the operation of the drying tower. With 24 operators and four shifts a day, the selection of lances operating within the tower varies greatly. This, along with the occurrence of overlap (especially overlap between top-layered lances), gives rise to colossal variation in the slurry coverage between shifts and operators. So one would like to minimise all overlap: overlap within a level is not necessary, it impacts very negatively on the efficiency of the tower, and it can easily be avoided.

The proposed solution will have *no* intra-layer overlap. This is especially helpful when one to 24 lances are operating in the tower. This is because, as long as only top layered lances are spraying, there will be no overlap. The only variable that must be considered by the operators is the symmetrical opening of the lances. This is important because the superheated air from the furnace is pumped into the tower symmetrically. If lances are operating in only one half of the tower, the hot air entering the opposite side of the tower will not directly dry out slurry, and will thus be wasted. With successful completion and implementation of the project, Unilever will undoubtedly experience a decreased – and more constant – use of gas within the furnace.

1.5 Project Aim

The aim of this project is to improve the efficiency of the tower through the best configuration of the lances, reducing the amount of gas used per time period to produce the desired amount of powder. Thus, the following are desired objectives:

- To save money
- To reduce environmental impact.

1.6 Project Scope

Initially, an in-depth literature review is done to research appropriate methodologies that will ultimately be implemented in the solution.

A basic simulation of the tower operations has been done using Microsoft Excel. Operations research has never been used by Unilever Boksburg in this context. Operations research may, however, be useful and practical in obtaining a solution. This is because there are tens (if not hundreds) of thousands of feasible solutions.

The project includes an operational study to determine the optimal positioning of top layer lances within the tower, as well as a mathematical positioning of the bottom layer of lances to reduce the number of open spaces within the tower. A comparison between current methods/operations and the proposed solution will be made, where slurry overlap and open spaces within the tower are compared. Validation of the proposed solution is also considered to be important, and will be included. The results obtained by the operational model will be tested in practice by Unilever, and, if Unilever feel that production could be positively affected by this project's findings, the findings will be implemented. Implementation of the results obtained will not form part of the project scope.

1.7 Deliverables

This project consists of five main deliverables, each with its own purpose and completion date. They are: the project proposal, interim project report, final project document, project poster, and the final project presentation.

A fully functional operations research model, with the accompanying results, is presented. The non-linear operations research model will focus on the configuration of the top layer of lances within the tower. The objective function is to maximise the area coverage in the tower. By maximising the cross-sectional slurry area covered, the open spaces will be minimised and tower efficiency will improve.

This model will provide invaluable information and insight to the company about improving the efficiency of the tower and furnace operations.

1.8 Project Plan

1.8.1 Activities and Tasks

Activities and tasks are to be completed within a specific period throughout the project's duration. This will ensure that the project and all deliverables are timeously completed. Some of the preliminary tasks include process familiarisation, as well as problem and scope definition. These preliminary tasks are highly time-consuming, but they are integral to the success of the project. All further work is based on a sound understanding of the process and the problem to be solved.

Chapter 2

Literature Review

2.1 Problem Identification

The Unilever energy balance project encapsulates two distinct sub-problems: Assigning the lance configuration and positioning within the drying tower, and determining how the tower should be operated in order to use gas more efficiently. The top layer lance assignment problem within the drying tower has been identified as a variation of the Circle Packing Problem.

2.2 Introduction to the Circle Packing Problem

The circle packing problem (CPP) is described thus by Lopez and Beasley (2010): "Finding the maximum radius of a specified number of circles that can be fitted, without any overlaps, into a two dimensional container of fixed size". Circle packing problems can be solved by using two distinct objective functions. First, one can aim to maximise the radius of a given number of circles within the containing shape of fixed size. Second, one can aim to minimise the size of the containing shape for a fixed number and radius of contained circles. The CPP has been used to solve problems of two and three dimensions, although when applied to the lance assignment problem, a two dimensional version will suffice.

The circle packing problem has been applied to a wide variety of industries and practical problems. According to Hifi and M'Hallah (2009), the CPP has been found to be applicable to an array of real-world problems including the textile, manufacturing, automobile, aerospace, forestry, logistics, food, and a variety of other industries. For example, solutions to CPP have been successfully used in logistics, where cylindrical shapes have to be optimally packaged into a container of fixed size. The CPP has also proven to be applicable to the manufacturing industry, specifically the automotive manufacturing industry, where the smallest possible hole needs to be drilled through which to squeeze a fixed number of identical wires. This is done to keep as much structural integrity as possible without harming wires.

Hifi and M'Hallah have classified CPPs as 'NP Hard' optimisation problems. An NP Hard is defined by Mathworld as follows: "A problem is NP-hard if an algorithm for solving it can be translated into one for solving any NP-problem (nondeterministic polynomial time). NP-hard therefore means 'at least as hard as any NP-problem', although it might, in fact, be harder."

CPPs have been solved by using a wide variety of algorithms, including computer-aided optimality proofs, branch and bound procedures, simulations, physical trial and error approaches, heuristics, and metaheuristics. The CPP is especially difficult to solve as the number of circles increases and when the container is circular. This is because the optimal solution may be unaffected by moving one or several of the contained circles. This is especially prevalent when a ‘rattler’ is present. Rattlers are defined as circles that are not fully constrained by other circles or the container, leaving them free to move within that space without affecting the optimality of the solution. Furthermore, it should be noted that (especially when the container is circular) the optimal solution can rotated without affecting the optimality of the solution. This provides an infinite number of optimal solutions.

According to Hifi and M’Hallah, the CPP can be classified as a mixture of a continuous and a discrete optimisation problem. This unusual phenomenon occurs because the positions of circles within the container are continuous, owing to the possible presence of rattlers as well as rotation, reflexion, and reordering of the optimal solution. However, the structure of circles within the container is considered to be discrete.

This has led to the use of algorithms that combine local, exact optimisation searches with heuristics. Cassioli, Locatelli, and Schoen explore this idea in their paper, “Dissimilarity measures for population-based global optimisation algorithms”.

This review will identify, discuss, analyse, and evaluate successful recent approaches to solving this problem.

2.3 Lance Assignment Problem

Within the tower, each lance produces a cone of slurry as it sprays out of the nozzle. When viewed cross-sectionally, these cones take on circular shapes within the circular tower. The circle packing problem will solve the above-mentioned problem by optimally arranging circles originating from the top layer of lances. This will ensure that in the top layer there is no overlap between cones from the top layer. Additionally, open spaces between the cones will be minimised.

2.3.1 Heuristic Algorithm of Birgin and Sorbal

Birgin and Gentil (2010) use the heuristic of Birgin and Sorbal (2008) to pack congruent circles within an assortment of two-dimensional containers: squares, circles, strips, rectangles, and equilateral triangles. The heuristic consists of non-linear equations, and applies the mathematical Newton-Raphson method, which improves upon the previous approximate optimisation with each consecutive iteration until the perceived optimal solution (local optimum) is found.

The heuristic algorithm of Birgin and Sorbal (2008) concentrates on the contact that the circles make with the other circles as well as with the container. Because this algorithm focuses on the contact of circles within the container, a problem arises whenever a circle does not make contact with other circles. These loose circles are called ’rattlers’. Birgin and Gentil improve the heuristic by incorporating a step that corrects the position of any overlapping circles.

Because the solution of the lance packing problem is not known, it would be risky to use this heuristic to solve the problem, as rattlers may be part of the solution. This would cause the runtime of the algorithm to increase.

2.3.2 Monotonic and Population Basin Hopping

In the *Journal of Global Optimisation*, Grosso et al. (2010) solve the problem of packing equal and unequal size circles into a circular container by using a monotonic and population hopping approach.

This heuristic does not focus on packing equal-sized circles into a container, and thus it might be unnecessarily complex, and have a negative influence on the time needed to run the algorithm. Ultimately, the simplicity of other algorithms makes them more understandable, and provides solutions in a shorter time.

2.3.3 Energy Landscaping Paving (ELP)

The ELP method was initially proposed by Hansman and Wille (2002), who combined the Tabu search created by Cvijovic and Klinowski (1995) and Besold et al. (1999) for energy landscape deformation. Lui et al. (2009) use the ELP heuristic algorithm to find the global optimum of packing circles into a circular container. Lui et al. (2009) improve on the original ELP algorithm by integrating a ‘configuration update mechanism’, which yields the improved energy landscaping paving algorithm, ELP+. The ELP+ algorithm can be used to solve a circle packing problem of packing up to 100 identical circles, 50 non-identical, and 50 identical spheres into a circular container. The ELP+ algorithm is an iterative approach; each iteration repositions the location of the centre of a chosen circle until the solution is found.

2.3.4 Formulation Space Search

The formulation space search (FSS) was initially applied to the circle packing problem by Mladenovic et al. (2005). Later, Mladenovic et al. (2007) improved on the initial heuristic by using both Cartesian and Polar coordinates to identify the positioning of the packing circles. The number of constraints were also reduced, making the solution more efficient.

Lopez and Beasley (2011) developed an altered and improved heuristic algorithm that was also based on FSS. The FSS uses different formulations of the same problem to obtain improved solutions when compared with singular formulation algorithms. FSS-based algorithms are especially suited to non-linear optimisation problems. This is because a change in the formulation of the problem will change the properties of the problem. This ultimately improves

the solution, because as a stationary point of one formulation is reached and the formulation of the problem is changed, the stationary point may be moved and improved upon. Mladenovic et al. and Lopez and Beasley exploited this characteristic of optimisation by defining the positions of some circles in Cartesian and others in Polar coordinates. Their algorithm then changes the circles that are expressed in Polar coordinates to Cartesian coordinates, and vice versa, with each iteration of the algorithm. By using this technique, Lopez and Beasley's heuristic improved on a number of previous 'optimal solutions' for certain containers. It should also be noted that they focused their efforts on the development of a solution for two dimensional containers – especially circular containers. Lopez and Beasley formulated the solution as follows:
Let

- **C** be the set of circles whose centres are expressed in terms of Cartesian coordinates, so for circle $i \in C$ its centre is at (x_i, y_i) in Cartesian coordinates.
- **P** be the set of circles whose centres are expressed in terms of Polar coordinates, so for circle $i \in P$ its centre is at (r_i, θ_i) in polar coordinates (where $C \cap P = 0$; and $C \cup P = \{1, . . . ,n\}$).
- Q be the set of all pairs $\{(i, j) \mid i = 1,. . . ,n; j = 1,. . . ,n; i \neq j\}$
- R be the radius associated with each of the *n* circles.
- $R_{overlap}$ be an upper bound on R, formally $R_{overlap}$ is the maximum radius that the circles can have before they must overlap due to area considerations, defined here by equating the area of the containing unit circle ($\pi 1^2$) to the total area of the *n* circles ($n\pi R^2_{overlap}$), so $R_{overlap} = 1/n^{0.5}$

Maximise $\boldsymbol{R}$		(1)
Subject to: $x_i^2 + y_i^2 \leq (1 - \boldsymbol{R})^2$	$\forall\, i \in \boldsymbol{C},$	(2)
$r_i \leq 1 - \boldsymbol{R}$	$\forall\, i \in \boldsymbol{P},$	(3)
$(x_i - x_j)^2 + (y_i - y_j)^2 \geq 4R2$	$\forall (i,j) \in \boldsymbol{Q}$ with $i \in \boldsymbol{C}\; j \in \boldsymbol{C}\; i < j,$	(4)
$(x_i - r_j \cos(\vartheta_j))^2 + (y_i - r_j \sin(\vartheta_j))^2 \geq 4R2$	$\forall (i,j) \in \boldsymbol{Q}$ with $i \in \boldsymbol{C}\; j \in \boldsymbol{P},$	(5)
$r_i^2 + r_j^2 - 2r_ir_j \cos(\vartheta_i - \vartheta_j) \geq 4R^2$	$\forall (i,j) \in \boldsymbol{Q}$ with $i \in \boldsymbol{P}\; j \in \boldsymbol{P}\; i < j,$	(6)
$-1 \leq x_i \leq 1$	$\forall\, i \in \boldsymbol{C},$	(7)
$-1 \leq y_i \leq 1$	$\forall\, i \in \boldsymbol{C},$	(8)
$0 \leq r_i \leq 1$	$\forall\, i \in \boldsymbol{P},$	(9)
$0 \leq \vartheta_i \leq 2\pi$	$\forall\, i \in \boldsymbol{P},$	(10)
$0 \leq \boldsymbol{R} \leq \boldsymbol{R}_{\mathbf{overlap}}$		(11)

(1) The objective function of the problem.

(2) Constraint ensuring that every circle is fully contained by the container circle. (Cartesian Coordinate System – Non-linear)

(3) Constraint ensuring that every circle is fully contained by the container circle. (Polar Coordinate System – Linear)

(4) Constraint ensuring that no overlap occurs between packing circles. (Cartesian Coordinate System – Non-linear)

(5) Constraint ensuring that no overlap occurs between packing circles. (Cartesian and Polar Coordinate Systems – Non-linear)

(6) Constraint ensuring that no overlap occurs between packing circles. (Polar Coordinate System – Non-linear)

(7) Limit the Variable of the x coordinate of Cartesian Coordinate System

(8) Limit the Variable of the y coordinate of Cartesian Coordinate System

(9) Limit the Variable of the radius of the packing circles

(10) Limit the Variable of angle of the packing circles; this stops equivalent solutions. (E.g. $\theta + k(2\pi) = \theta$)

The pseudo-code for Lopez and Beasley's FSS algorithm is given below.

Algorithm 1: Formulation Space Search pseudo-code

Initialisation: $\Delta \leftarrow \frac{2}{3}R_{overlap}$ $R_{best} \leftarrow 0$ $t \leftarrow 0$

Randomly generate an initial solution

Iterative Process:

WHILE not termination condition **do**

$Q \leftarrow$ OverlapSet($X, Y, \Delta, R_{overlap}$)	{Find Overlap Set Q}
Solve NLP (x^0, y^0, C, P, Q, X, Y, Δ, $R_{overlap}$) to give (x,y)	
R* Correction (x, y, x, y)	{Correct radius}
$R_{best} \leftarrow \max\{R_{best}, R^*\}$	{Update R_{best}}
If $R^* \leq 0.001$ $\Delta \leftarrow \frac{1}{10} R_{overlap}$ else $\Delta \leftarrow \frac{2}{3} R^*$	{update Δ}
$t \leftarrow t + 1$	{update interation counter}
$C \leftarrow P$ $P \leftarrow \{1,\ldots,n\}C$	{Swop the sets of C and P}
$(X, Y) \leftarrow (x, y)$	{set (X,Y) to current solution}

End While

The pseudo-code provides a condensed yet simple explanation of an algorithm. The pseudo-code still makes use of conventional programming language; however, its purpose is to inform readers of the operation of the algorithm. The pseudo-code is not intended for computational reading.

From the pseudo-code above, the initial step is to generate a random solution for the circle packing problem. One can notice that various items within the While loop have not been defined in the pseudo-code.

- *OverlapSet (Q):* The overlap set refers to a procedure that reduces the number of non-linear constraints that will need to be performed to ensure that overlap does not occur between packing circles. This involves performing calculations that will determine whether certain packing circles could overlap. This is accomplished by allowing the circles to move within a defined area to establish whether overlap is possible.
- *NLP:* Non-linear optimisation Problem describes the following constraints: $\{X_i - \Delta \leq x_i \geq X_i + \Delta\}$ & $\{Y_i - \Delta \leq y_i \geq Y_i + \Delta\}$. Delta has been defined in the initialisation phase.
- *Correction:* The correction step of the algorithm has a dual purpose. First, it ensures that all packing circle centres are fully contained. Second, a constant radius is established for all packing circles such that no overlap occurs between packing circles or with the container.
- R_{best}: This step chooses the maximum radius when comparing the radius obtained from the current iteration with the radius from the previous iteration. Thus, when numerous iterations of the algorithm are completed, the optimum solution will eventually be reached and thus will not change.

The FSS of Lopez and Beasley provides the best solutions for two dimensional containers in a time efficient manner. It should also be noted that Lopez and Beasley's paper on circle packing is the most recent study done on the subject.

2.3.5 TomSym Modelling

The circle packing problem is explored by TomSym modelling. TomSym is a TOMLAB class used to model optimisation and constraint problems in MATLAB. According to the TomSym website (www.tomsym.com), this class has the ability to solve linear, non-linear, and mixed-integer problems. The non-linear problem-solving ability is of particular interest due to the non-linear nature of circle equations, which is key to finding the solution to the CPP.

TomSym explores the circle packing problem by inscribing a polygon within a circle. TomSym uses the logic that by making the number of sides of the inscribed polygon arbitrarily large, this shape will represent the perfect inscribing circle. The pseudo-code for the TomSym solution is given below.

Algorithm 2: TomSym solution pseudo-code

Input:	Number of sides of the polygon
	Number of packing circles
	Number of iterations (number of different starting positions)
Output:	Coordinates of the packed circles
	Radius of the packed circles
Step 1:	Calculate angle from origin, covered by each side of the polygon
Step 2:	Calculate distance from the origin to the midpoint of the side of the polygon.
Step 3:	Ensure all circles are within the container.
Step 4:	Ensure no overlap occurs between circles.
Step 5:	Start with a random solution.
Step 6:	Solve by maximising radius.
Step 7:	Plot solution

By increasing the number of sides of the polygon, its shape changes, becoming more circular. The more circular the polygon's shape, the more accurate the solution becomes. There is a relationship between the number of iterations performed and the accuracy of the solution. However, as one increases the number of sides of the polygon and the number of iterations performed, the running time of the program may be affected drastically.

The TomSym example provides an efficient, simple, easily understood solution. The MATLAB coding for this program is given in appendix H.

2.3.6 Packomania Website

The Packomania website was established in 1999. It contains all the best, *known* solutions of a wide variety of circle packing problems, and is updated whenever an improved solution is found. Packomania container shapes include circles, semicircles, squares, rectangles, and triangles. Solutions for circular shaped containers are given from two packing circles up to 1,100 packing circles. This site is widely considered to be the 'gold standard' for comparing solutions and for establishing the viability of a solution.

The information obtained from this site will be used as a starting point in the search for a solution to the lance assignment problem. The positions of the current best, known solution for circles will be adopted as the random starting point when using the heuristic developed by Lopez and Beasley.

2.4 Excel Simulation of Lance Positioning

Microsoft Excel has long been successfully used as a tool to simulate Monte Carlo experiments. Monte Carlo simulations are defined by Investopedia as "a problem solving technique used to approximate the probability of certain outcomes by running multiple trial runs (simulations) using random variables".

A.M. Brown (1997) developed a method of simulating biological systems using Excel. In-cell formulae were used, into which data could be put to provide a required output. The outputs from the formulae were then available for use as inputs in other sections of the simulation. According to Brown, Excel is an effective tool for simple simulations because one does not need to learn a programming language, nor the specialised skills that are required to use other simulation programs.

Because it is widely available and user-friendly, Microsoft Excel has been used in a wide range of study disciplines, from medicine to engineering, to simulate scenarios. Excel was used by I. Meineke and J. Brockmöller to simulate pharmacokinetic models; and they commented on Excel's versatility and simplicity. Brown used Excel to simulate biological systems. R.J.W. Lambert et al. used Excel for a Monte Carlo non-linear regression analysis by incorporating the Excel solver and various add-ins. A range of other studies have also made use of Excel as a simulation program.

Similarly, Excel has been identified as an appropriate and easy-to-use tool to simulate lance positioning within the tower. Its ease of use, availability, and ability to produce sufficient graphical simulation made it the obvious choice to illustrate the positioning of lances and slurry coverage within the tower.

2.5 Change Management

At its core, this project is about managing change effectively to improve a process within a business. So it is pertinent that change management should be defined and well understood in order to undergo a proposed change successfully.

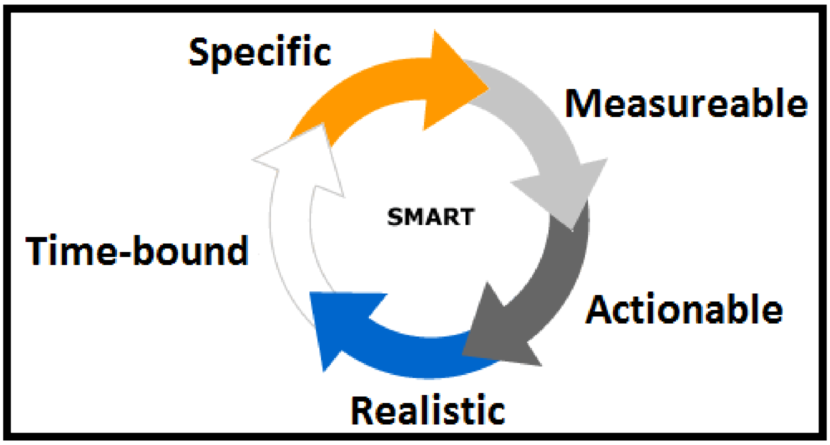

Figure 5: Graphical illustration of SMART change

Changes to a process within an organisation should be defined according to the SMART model (TOGAF Reference model, Version 8.1.1 2007). The proposed change to the tower is 'SMART':

- ***S****pecific*
- ***M****easurable*
- ***A****ctionable*
- ***R****ealistic*
- ***T****ime-bound*

Specific: The change to the lance positions within the tower should be defined according to a specific set of objectives. (These objectives have been thoroughly discussed in Chapter 1.)

Measureable: The final savings of gas will not be measurable until the improved lance positioning has been implemented. The decrease in overlap and open spaces, however, are measureable.

Actionable: The change should be actionable in that each person affected by the change should be informed of the change and how it will affect their roles and responsibilities. This is particularly applicable to the operators of the drying tower.

Realistic: The increase in the furnace's productivity is realistic, given the feasibility of the study.

Time-bound: Change should always have a specific date when the proposed change would be considered for implementation. In this case, the date is 13 October 2011 – the final submission date for this report.

By making use of the SMART model, many potential problems are avoided before they can affect the project. The SMART model also ensures that the change will have a definite, positive impact within a certain time period. This ensures that the project will be completed within the specified time frame.

If the proposed change is badly presented, it will not be implemented. However, if it is presented well but poorly executed, the change might be implemented with devastating effects on the system. This report aims to ensure that both presentation and execution achieve levels of excellence.

Chapter 3

Solution Approach

3. 1 Attribute Identification

When studying the operations of the lances within the tower, it is vitally important that the attributes of the spraying lances are identified. By doing so, one can accurately simulate the spray pattern within the tower. The following attributes were identified:

- Lance position
- Spray cone angle
- Nozzle angle

The two-dimensional position of any lance can be described by using two pieces of information: the length of the lance and the angle. This is illustrated in Figure 6 below. The method used to identify the position of the lance is similar to the Polar co-ordinate system. There are two slight differences, both stemming from the fact the reference point is not the origin (Cartesian coordinates (0;0)), but the containing wall of the drying tower. The length of the lance is measured from the wall towards the centre. The angle is measure from the left side of the tower in an anti-clockwise motion. The Polar co-ordinate system uses the origin as reference point for the length (called radius) and measures the angle in an anti-clockwise direction.

The rationale behind this altered coordinate system is that it provides a better understanding of exactly where the lance is positioned within the tower. Additionally, Unilever used this system when designing an Excel simulation of the lances within the tower. Thus, by using the same system, no conversions would need to be made when using the Excel simulation. The coordinates will be given as follows: $(l;\vartheta)$. The final solution will, however, be provided in Cartesian coordinates, following the convention.

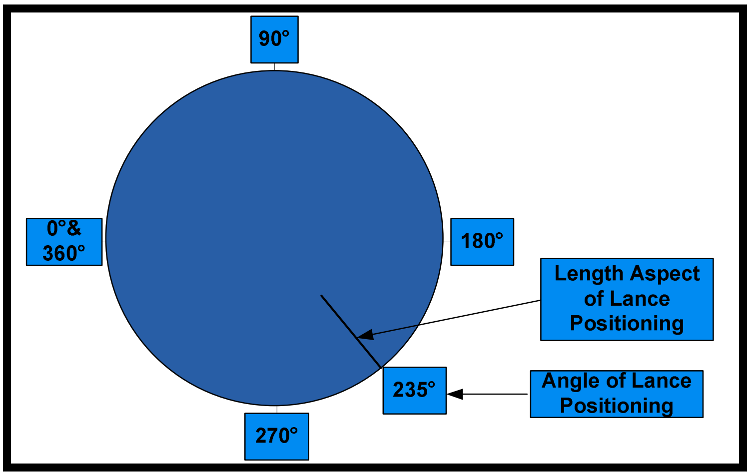

Figure 6: Illustration of coordinate system used

When describing the positioning of lances, one must always take in account that there is a third dimension, because there are two layers of lances within the tower.

The spray cone angle (SCA) is defined as the angle of slurry formed as it sprays from the nozzle at the end of the lance. This attribute is affected by the pressure of the slurry and by the type of nozzle used. At the current pressure of the slurry and nozzles used, which remains constant unless changed by Unilever management, this angle has been measured at 61°.

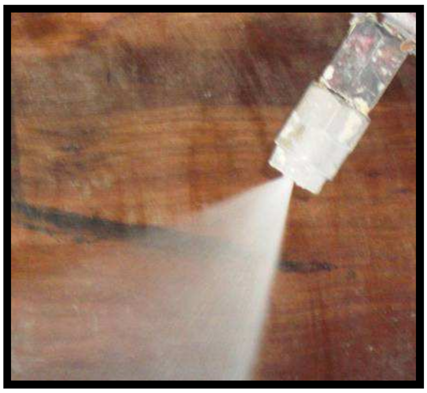

Figure 7: Photographic representation of lance nozzle spraying slurry at an angle of 61°

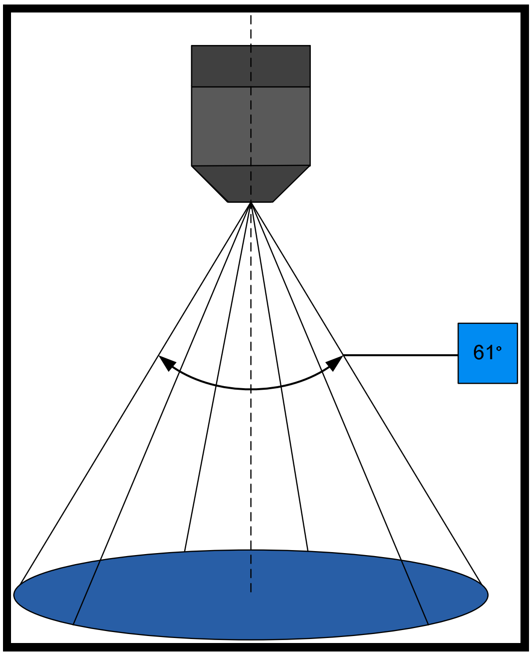

Figure 8: Graphical representation of lance nozzle spraying slurry at an angle of 61°

The SCA is affected by gravity within the tower. The effect is that the slurry cone 'tapers' off as the slurry falls. This occurs because, as soon as it leaves the nozzle, there is no longer a force pushing it outwards, but the force of gravity continues to act downwards. So the further the slurry moves from the nozzle, the more distorted the shape of the cone becomes. This is illustrated in Figure 9 below. This aspect is very important when calculating the surface area of the slurry within the tower. The further the vertical distance between the nozzle and the location of the simulated slurry coverage, the less accurate the simulated coverage will be. This phenomenon is dealt with by measuring the maximum diameter attained with the effect of tapering, and converting this value to the vertical distance from the lance without the effect of tapering. This vertical value was found to be 1.35 metres. It should be noted that, although the initial angle is 61°, as tapering occurs, the actual angle becomes smaller as tapering becomes more prevalent. The diagram in Figure 9 illustrates this effect.

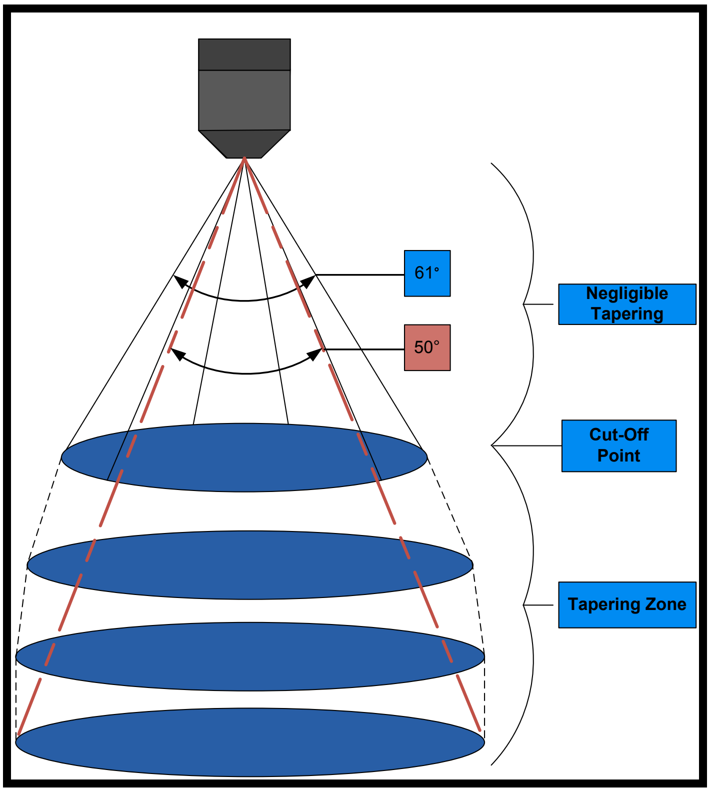

Figure 9: Graphical illustration of tapering of slurry fall

The nozzle angle refers to the angle at which the nozzle is positioned at the end of the lance. This angle has an influence on the cross-sectional shape of the slurry as it falls. Figure 11 illustrates different nozzle angles.

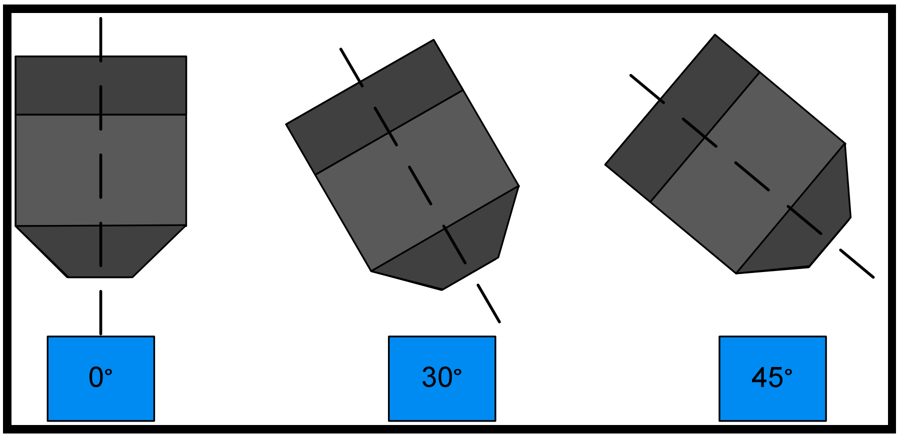

Figure 10: Illustration of nozzle angle changes

The greater the nozzle angle, the greater the impact on the slurry flow. The closer the angle is to 0°, the more circular the cross-sectional slurry pattern will be. When the angle is increased, an elliptical shape is formed. This is illustrated in Figure 11 below. Currently all upper level lances are at a 35° angle, while all lower level lances are at a 4° angle. Even with a 35° angle, the cross-sectional view of the slurry still proves to be largely circular. Thus, for the sake of simplicity, these areas will be regarded as circular, not elliptical.

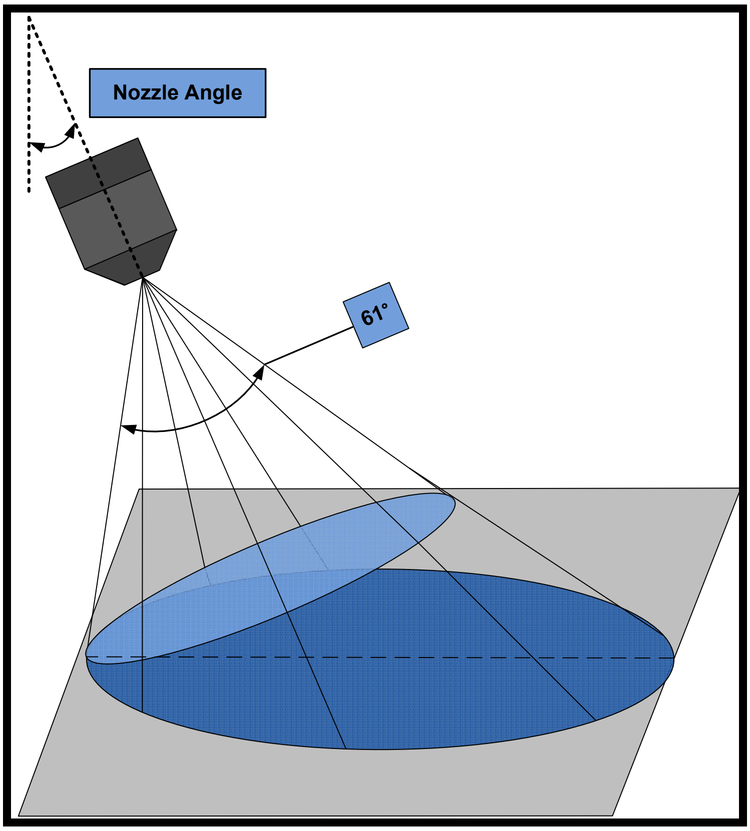

Figure 11: Graphical representation of nozzle angle and the resulting distortion of the cross-sectional view of the cone

The proposed solution will only make use of circles. This forces the nozzle angles to be 0°. This is done for two reasons. The first is for the sake of simplicity. Thus far, not much study has been done on the packing of ellipses, largely due to the fact that there are not many applications where ellipses will be packed in a container. Calculating their area and modelling elliptical shapes would also add an unnecessary complication to an already challenging problem. Second, by setting the nozzle angles at 0°, the slurry density will be more even within the cone. This will promote a more even drying of the falling slurry. The nozzle angles are currently positioned at 35° to reduce the overlap of falling slurry and to compensate for a large open space in the centre of the tower.

3.1.2 Classification of Overlap

When it comes to overlapping slurry, not all overlap is considered equally detrimental to the drying of the slurry into powder. This is because some overlap is largely unavoidable, while other overlap can be easily avoided. Overlap that is easily avoided is thus considered to be more detrimental than unavoidable overlap. Three factors need to be taken into account when classifying the severity of the overlap:

- Intra- / inter-layer overlap

  Intra-layered overlap refers to overlap that occurs within a layer of lances – i.e. two top layered lances' slurry cones overlapping – while inter-layer overlap refers to overlap between the two layers of lances. Overlap between layers should be expected, especially in the proposed solution. This is because only the top lance layer will be optimised, and the bottom layer lances will be positioned in the gaps created by the top lances.

- Area of overlap

  The area of overlap refers to the extent of overlap between slurry cones. The greater the area of slurry cone overlap, the more detrimental will be the effect on the drying capability of the superheated air. Thus the area of overlap between cones should be minimised.

- Number of overlapping cones (cross-sectionally represented as a circle.)

  The number of overlapping cones has an impact on the slurry density and thus the drying ability of the slurry. This effect is illustrated on page x figure y.

The combination of these three factors has led to the decision that overlap should be classified. By classifying the types of overlap, a fair comparison can be made between the current and the proposed positioning of lances. Taking all three aspects into account produces the following classification system:

First degree overlap: First degree overlap (FDO) is defined as overlap that occurs between three slurry cones, including all bordering slurry between any two of the three cones. First degree overlap will always be a combination of intra- and inter-layered overlap. First degree overlap severely disrupts the flow and density of slurry within the tower, with a significant impact on the PMC and power quality. Figure 12 illustrates an example of FDO: blue circles represent slurry cones originating from top layered lances, while red circles represent cones originating from bottom layered lances. It is important to note that, because of the presence of a third overlapping circle, the overlap between any two of the three circles is considered to be FDO.

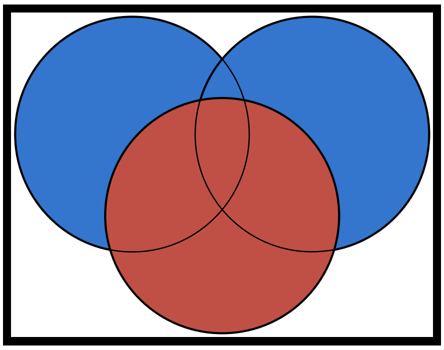

Figure 12: Graphical representation of an example of first degree overlap

Second degree overlap: Second degree overlap (SDO) is defined as any intra-layered overlap, regardless of the size of overlap. This classification system does not take the size of this overlap into account, because all intra-layered overlap is avoidable. Figure 13 illustrates SDO.

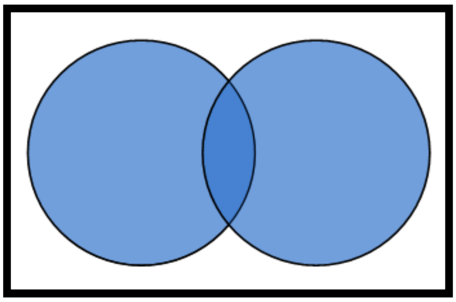

Figure 13: Graphical representation of an example of second degree overlap

Third degree overlap: Third degree overlap (TDO) refers to any inter-layered overlap. The third degree overlap will be ranked according to the area of the overlap. Figure 14 shows an example of TDO, which is overlap between cones originating from different layered lances.

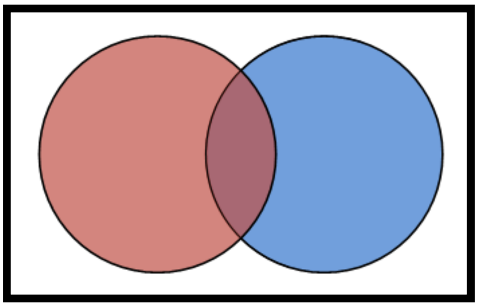

Figure 14: Graphical representation of an example of third degree overlap

3.1.3 Classification of Open Spaces

As with overlap, not all open spaces within the drying tower are considered equally detrimental to the slurry drying process. However, there are only two factors to take into consideration when classifying the severity of open spaces.

- Size

The larger the size of the open space, the more superheated air will 'escape' through space. This will lead to inefficiency within the tower.

- Shape

The more circular the shape of the open space, the easier it is to remedy the predicament by simply positioning another lance at the centre of the opening.

The combination of these factors leads to this classification of open spaces within the tower:

First degree spaces: First degree spaces (FDS) are defined as circular-shaped spaces that can accommodate at least 80% of a lance cone. FDS should not be present, as the amount of neglected coverage has too severe an impact on the amount of escaped air.

Second degree spaces: Second degree spaces (SDS) are classified by their irregular shapes and relatively small surface area. Gaps occurring directly next to the drying tower are considered unavoidable and negligible.

Third degree spaces: Third degree spaces (TDS) are defined as small spaces that are unavoidable when packing circles. These spaces are generally convexly triangular-shaped, and are formed when three circles are tightly packed. TDS also occur adjacent to the tower wall.

By having a classification system for the open spaces within the tower, the current system can be easily compared to the proposed lance configuration.

3.2 Solution Explanation

The initial step in solving the lance positioning problem is to choose the correct algorithm. The improved formulation space search by Lopez and Beasley (2010) was found to provide the best theoretical solution to the lance positioning problem. The TomSym example of the circle packing problem was also identified as a high-quality solution to the problem. It was decided that these two methods were the best to use, given the software they use and the results they obtain. Both of the above-mentioned solutions require the use of MATLAB 7 and the add-in SNOPT (Sparse Nonlinear Optimiser) developed by TOMLAB.

Once the solution is found, it is important to recognise that the solution is given for a unit circle – i.e. a circle with a radius of one. All results should then be transformed to apply to a nine metre diameter circle. Even though the size will be different, the position of the contained circles will remain unchanged. For the conversion from the unit circle to the nine metre diameter circle, either Polar or Cartesian coordinates may be used. In Polar coordinates, the conversion of container circle size will have an impact on the radius, but not on the angle. This concept is illustrated in Figure 15 below. Alternatively, when using Cartesian coordinates, the circle centre and the radius of each circle are altered by simply multiplying by the increase in radius – in this case, 4.5.

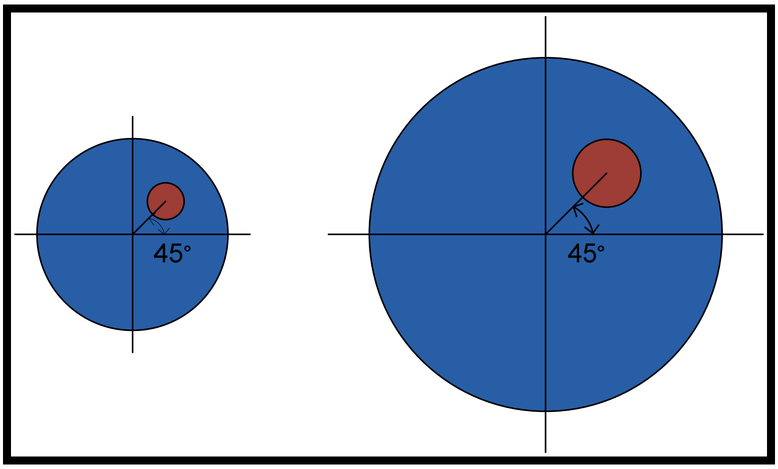

Figure 15: Graphical representation of effect of increasing the scale of solution

Once the positioning of the lances has been completed for the circle with a radius of 4.5 metres, a comparison of the differing configurations will be done.

The radius of the slurry circles within the tower will provide the necessary information to calculate the vertical distance from the lance. If this distance is too great, tapering of slurry comes into play, thus rendering the solution inaccurate. It has been established that the maximum radius attained by falling slurry after tapering is equivalent to the radius at a vertical distance of 1.35m below the lance when tapering is not taken into account. This will be the reference point for all calculations of overlap within the tower.

The number of top lances is restricted to 24 for a number of reasons. First, increasing the number of top lances beyond 24 makes maintainability problematic. Second, Unilever have stated that for operational reasons the number of lances per layer should not be altered.

The results are simulated in Microsoft Excel and MATLAB, providing a clear view of where the remaining open spaces within the tower are. As a total of 42 lances must be positioned within the tower, the remaining number of lances (42-24=18) will then be positioned in the bottom layer of lances in the largest of the open spaces within the tower. Following the positioning of the bottom layered lances, the solution, and the current lance positioning, are simulated. Overlap and open space are then measured according to the classifications mentioned above. A thorough comparison of the different set lance positioning is completed. A wide variety of tools is used to illustrate the comparison successfully and efficiently.

Following the in-depth comparison (development of business case), an informed decision can be made by Unilever about implementing the project.

Chapter 4

Model Execution and Comparison

4.1 Operations Research Solution

The operations research model developed by Lopez and Beasley (2010) is constructed with the use of MATLAB, along with the add-in SNOPT developed by TOMLAB.

Maximise $\boldsymbol{R}$		(1)
Subject to: $x_i^2 + y_i^2 \leq (1 - \boldsymbol{R})^2$	$\forall\ i \in \boldsymbol{C},$	(2)
$r_i \leq 1 - \boldsymbol{R}$	$\forall\ i \in \boldsymbol{P},$	(3)
$(x_i - x_j)^2 + (y_i - y_j)^2 \geq 4R2$	$\forall (i,j) \in \boldsymbol{Q}$ with $i \in \boldsymbol{C}\ j \in \boldsymbol{C}\ i < j,$	(4)
$(x_i - r_j \cos(\vartheta_j))^2 + (y_i - r_j \sin(\vartheta_j))^2 \geq 4R2$	$\forall (i,j) \in \boldsymbol{Q}$ with $i \in \boldsymbol{C}\ j \in \boldsymbol{P},$	(5)
$r_i^2 + r_j^2 - 2r_ir_j \cos(\vartheta_i - \vartheta_j) \geq 4R^2$	$\forall (i,j) \in \boldsymbol{Q}$ with $i \in \boldsymbol{P}\ j \in \boldsymbol{P}\ i < j,$	(6)
$-1 \leq x_i \leq 1$	$\forall\ i \in \boldsymbol{C},$	(7)
$-1 \leq y_i \leq 1$	$\forall\ i \in \boldsymbol{C},$	(8)
$0 \leq r_i \leq 1$	$\forall\ i \in \boldsymbol{P},$	(9)
$0 \leq \vartheta_i \leq 2\pi$	$\forall\ i \in \boldsymbol{P},$	(10)
$0 \leq \boldsymbol{R} \leq \boldsymbol{R}_{\mathbf{overlap}}$		(11)

Algorithm 1: Formulation Space Search pseudo-code

Initialisation: $\Delta \leftarrow \frac{2}{3} R_{overlap}$ $R_{best} \leftarrow 0$ $t \leftarrow 0$

Randomly generate an initial solution

Iterative Process:

WHILE not termination condition **do**

$Q \leftarrow$ OverlapSet($X, Y, \Delta, R_{overlap}$) {Find Overlap Set Q}

Solve NLP (x^0, y^0, C, P, Q, X, Y, Δ, $R_{overlap}$) to give (x,y)

R* Correction (x, y, x, y) {Correct radius}

$R_{best} \leftarrow \max\{R_{best}, R^*\}$ {Update R_{best}}

If $R^* \leq 0.001$ $\Delta \leftarrow \frac{1}{10} R_{overlap}$ else $\Delta \leftarrow \frac{2}{3} R^*$ {update Δ}

$t \leftarrow t + 1$ {update iteration counter}

$C \leftarrow P$ $P \leftarrow \{1,\ldots,n\}C$ {Swop the sets of C and P}

$(X, Y) \leftarrow (x, y)$ {set (X,Y) to current solution}

End While

The model, along with the accompanying iterative procedure, illustrated by the pseudo-code above is discussed in the literature review, and has been constructed. Appendix G shows the FSS coding.

Initialisation is the first step of the FSS algorithm. This step requires a random generation of positions of circles. This randomly-generated solution is then improved during subsequent iterations. Information on the current best known solution for the packing of 24 circles was used as the initial random generation of a solution. This is done in an attempt to improve on the current best known solution. However, the solution obtained by this model was not as accurate as expected. This unforeseen situation led to the use of a different technique to solve the problem.

Thus an additional MATLAB model, developed and constructed by TomSym, was also used to model the problem. The TomSym solution proved to be much more time efficient, providing a better solution in a shorter time. The TomSym example model was run for a polygon with 1,500 sides, which provides the optimal positioning for the top lance layer. The positioning of the bottom layered lances was calculated using a variety of trigonometric and geometric equations and rules, in order to reduce the number of open spaces while avoiding overlap. The process of establishing the bottom lance positions is described in Appendix D.

4.2 Analysis of Current Configuration

The analysis of the current positioning of lances is subdivided into two distinct sections: first, the analysis of the overlap between slurry cones, and second, the analysis of the open spaces within the tower. The analysis is accurately executed through the use of the classifications of overlap and free space described in Chapter 3.

4.2.1 Overlap Analysis

The current lance positioning within the drying tower is symmetrical and highly complex. The symmetry of the configuration is aesthetically pleasing, as illustrated in Figure 3 above and Figure 16 below. The complexity is as a result of the nozzles of the top layered lances being angled at 35°, creating a distortion of the preferred circular cross-section, as mentioned earlier. To simplify the overlap calculations, the positions and nozzle angles were slightly altered to produce a circular cross-sectional view. The effects of the changes are shown in Figure 16 below. For the lance numbering, refer to Appendix C.

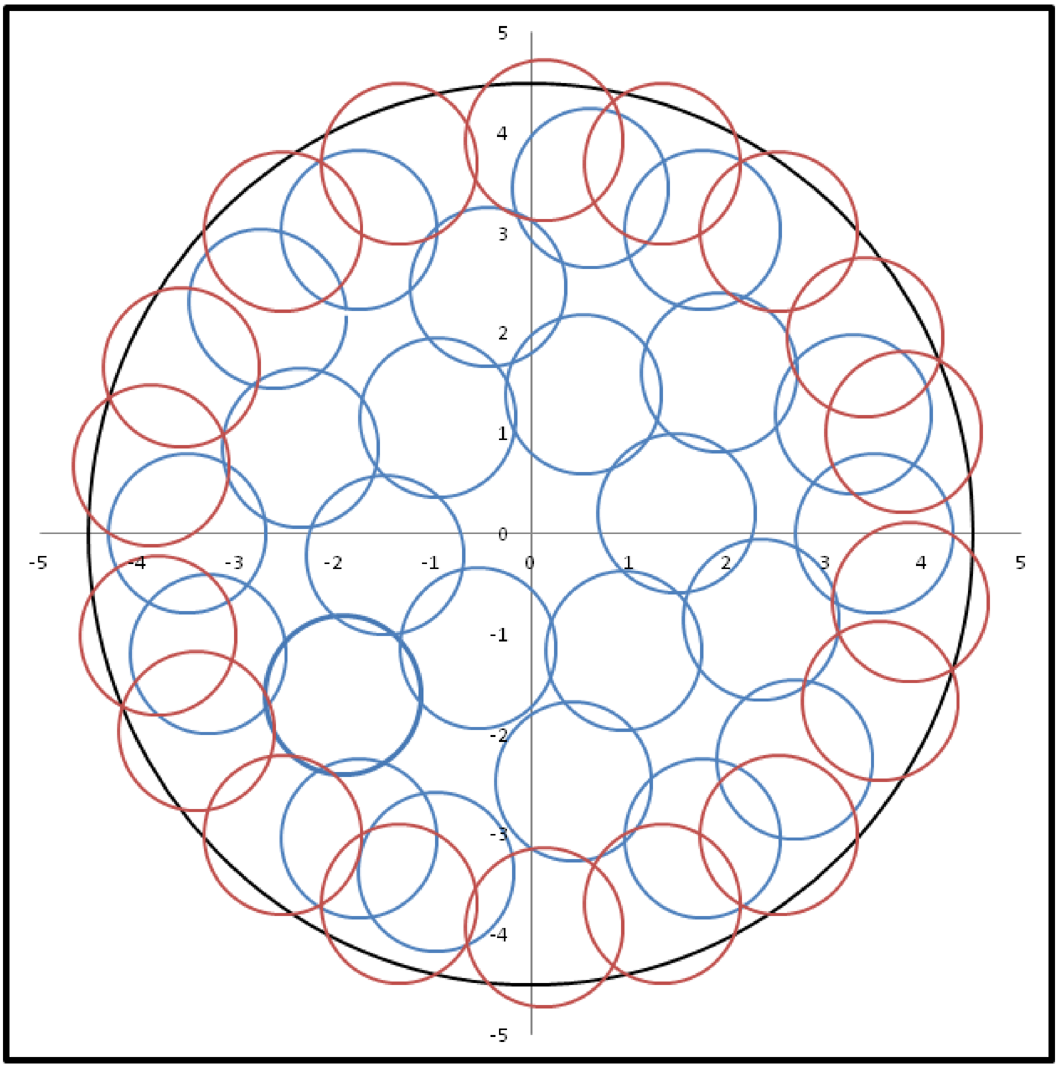

Figure 16: Revised current lance configuration, so that it is circular

With a circular cross-sectional view of falling slurry, overlap calculations are not difficult to calculate accurately. These calculations are set out in Appendix E.

At the outset of overlap analysis, it is important to gain a thorough understanding of the available cross-sectional area within the tower. This initial understanding will allow an effective analysis of the slurry overlap measurements within the tower. The cross-section of the tower is a perfect circle; thus the available area for the falling slurry is calculated as follows:

Area of a circle = πr^2 where r = 4.5m

= $\pi(4.5)^2$ = 63.617 m^2

The current total overlap within the tower was calculated to be 26.033m^2. This was done by adding all overlap within the tower, causing the overlap value to be slightly inflated. This happens when more than two circles overlap at the same position within the tower, and that particular area of overlap is measured twice. Exactly the same method of overlap calculation is used to calculate the proposed configuration's overlap. This is done to ensure consistent results and a fair comparison between the current and the proposed configuration. This trend is further explained in the analysis of FDO, and is schematically illustrated in Figure 17.

There are 68 instances of overlap in the current configuration of lances. An instance of overlap is defined as an event where slurry originating from a particular lance intersects the flow of slurry originating from a different lance. Lance number one has five instances of overlap, occurring with slurry flow originating from lances 12, 13, 25, 26, and 42. This overlap can be examined in Appendix C.

It is now pertinent to distinguish between an *instance* and an *occurrence* of overlap. An *instance* of overlap occurs between any two lances, as described above. An *occurrence*, however, is strictly linked to the degree of overlap. In FDO, there are generally three instances of overlap per occurrence. For example, lances 1, 12, and 42 overlap; this is categorised as one occurrence of FDO. Within this one occurrence there are three instances of overlap: 1 and 12, 12 and 42, and 1 and 42.

When overlap is measured, it is important that only one pair of overlaps should be measured. For example, slurry flow originating from lances 2 and 3 overlaps. From Table 1 below, this instance of overlap can be read as 'circle 2 overlaps with circle 3' and 'circle 3 overlaps with circle 2'. This instance of overlap should only be measured once to prevent the duplication of overlap measurements. Table 1 below illustrates this point in matrix format.

Duplication of overlap avoidance					
	1	2	3	4	5
1	0	0	0	0	0
2	0	0	0.321534	0	0
3	0	0.321534	0	0	0
4	0	0	0	0	0.321534
5	0	0	0	0.321534	0

Table 1: Illustration of overlap duplication avoidance

Note how the values above and below the pale blue diagonal line are equal. To curb the duplication, only values below the light blue diagonal line will be taken into consideration when calculating overlap.

First Degree Overlap: All overlap within the tower is first considered for FDO. Only if the overlap does not fall into this classification will the overlap be categorised into either SDO or TDO. Any instance of overlap that is classified as FDO will not be considered for either of the other two categories.

The FDO within the tower is calculated by adding the overlap between all the circles involved with FDO individually. This will lead to an inflated overlap figure, as illustrated by Figure 17 below.

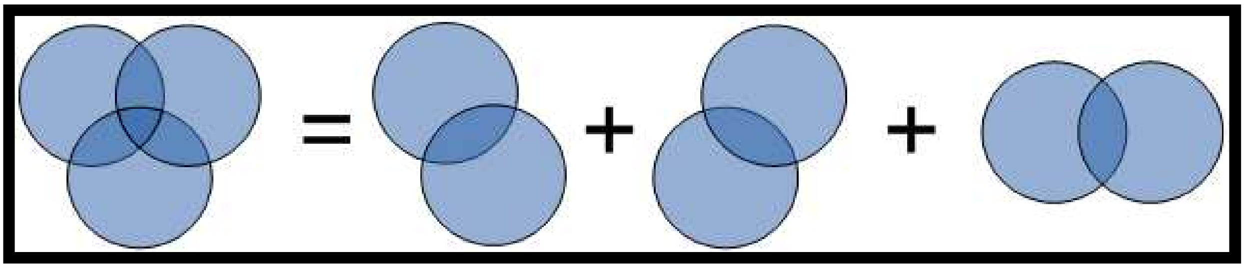

Figure 17: Illustration of FDO calculation

While some would argue that this method is inaccurate, it is used to calculate FDO for two reasons: first, it is simple to calculate, and second, it serves as a penalty for allowing FDO within the configuration of lances. The area where triple overlap occurs will experience three times the density of slurry compared with areas where no overlap occurs; and this will lead to severely uneven drying in the affected region. In additional, the same method will be used to evaluate the proposed solution, thus ensuring a fair comparison of the configurations.

Table 2 below illustrates the details of FDO in the current configuration of lances. Notice that occurrences 2 and 3 both include lances 3 and 27. The overlap occurring from these particular lances will only be calculated in occurrence 2, not in occurrence 3. This is evident when comparing the magnitude of overlap occurrences 2 and 3.

First Degree Overlap		
Occurrence	Lances	Area
1	1; 12; 42	1.845
2	2; 3; 27	1.867
3	3; 27 ;28	0.926
4	4; 29; 30	1.999
5	4; 5; 30	1.065
6	5; 30; 31	0.926
7	6; 32; 33	2.425
8	6; 7; 33	0.698
9	8; 9; 36	1.868
10	9; 36; 37	0.925
11	10; 11; 39	2.701
12	11; 39; 40	0.926
13	12; 41; 42	1.278
Total		19.458

Table 2: Table showing occurrence and area (m^2) of FDO

There are 13 occurrences of FDO within the drying tower, which equate to 32 instances of overlap within this classification.

Second Degree Overlap: If any overlap between lances falls into the FDO classification, this overlap should not be included in the SDO classification, because this would result in a duplication of measurements that would produce inaccurate results. Similarly, if an instance of overlap has been identified as either FDO or SDO, this instance cannot be considered for TDO.

Details of SDO are given in Table 3 below. There are 35 occurrences of SDO, translating into 35 instances. The occurrences and instances are identical owing to the characteristics of SDO, which is defined as any overlap occurring between two slurry circles originating from the same layer of lances. Thus, because only two slurry circles overlap, there is only one area of overlap – that is, one instance.

Of the 35 occurrences of SDO, 30 result from lances in the top layer overlapping, and the remaining five from bottom layered overlap. This trend is caused because the majority of intra-layer overlap in the bottom layer also overlaps with slurry originating from the top layer. The addition of this third overlapping circle results in the overlap being classified as FDO. When this occurs, the remaining intra-layered overlap within the bottom layer is limited to 5 occurrences. In addition, the top layer has 24 lances, while the bottom has only 18 lances. This contributes to the above-mentioned gap in occurrences between the layers. Lastly, the bottom layer only has lances positioned around the outside of the tower, while the top layer is more evenly distributed. This even distribution in the top layer results in small areas of overlap between a large number of lances, so that there is more than twice the amount of SDO than FDO. The total area of SDO, however, is only 18% that of FDO. This is illustrated in Table 3 below. Appendix C diagrammatically illustrates the positioning of lances and the respective coverage within the tower. These figures, along with Table 3, offer insight into the overlapping areas of slurry.

A thorough analysis and comparison of the classifications of overlap is done, following the explanation of TDO within the current configuration of lances.

Second Degree Overlap					
Occurrence	**Lances**	**Area**	**Occurrence**	**Lances**	**Area**
1	13; 19	0.069	**19**	12; 18	0.073
2	14; 19	0.102	**20**	25; 26	0.476
3	14; 20	0.069	**21**	31; 32	0.124
4	15; 20	0.102	**22**	34; 35	0.476
5	15; 21	0.053	**23**	37; 38	0.249
6	16; 21	0.120	**24**	40; 41	0.124
7	16; 22	0.069	**25**	18; 23	0.059
8	17; 22	0.102	**26**	18; 24	0.053
9	1; 13	0.073	**27**	13; 24	0.120
10	2; 13	0.073	**28**	19; 20	0.032
11	3; 14	0.073	**29**	20; 21	0.021
12	4; 14	0.073	**30**	21; 22	0.045
13	5; 15	0.073	**31**	22; 23	0.042
14	6; 15	0.073	**32**	23; 24	0.155
15	7;16	0.073	**33**	19; 24	0.045
16	8;16	0.072	**34**	28; 29	0.032
17	9; 17	0.073	**35**	38; 39	0.032
18	11; 18	0.073	**Total**		**3.569**

Table 3: Table showing occurrences and area (m^2) of SDO

Third Degree Overlap: The majority of overlapping circles have already been identified as either FDO or SDO. This leaves the remaining overlap to be classified as TDO. There are 17 occurrences of TDO, equating to 17 instances of overlap. The total area of overlap resulting from these 17 instances is small compared with FDO, and similar to the area of coverage of SDO.

TDO is defined as inter-layered overlap. Thus TDO should always be expected when packing two or more layers of circles into any container. TDO will result when an attempt is made to reduce the effect of free spaces, which is seen as more detrimental to the efficiency of tower operations than the effect of small amounts of TDO.

This principle is shown diagrammatically in Figure 18 below. The blue circles represent the slurry flow from top layered lances, and the red circles the bottom layered lances. Note that if the red circles were absent, there would be large gaps in the slurry flow, resulting in a significantly inefficient use of gas. TDO is thus deemed to be a ‘necessary evil’. The concept of balancing free spaces and overlap is addressed later.

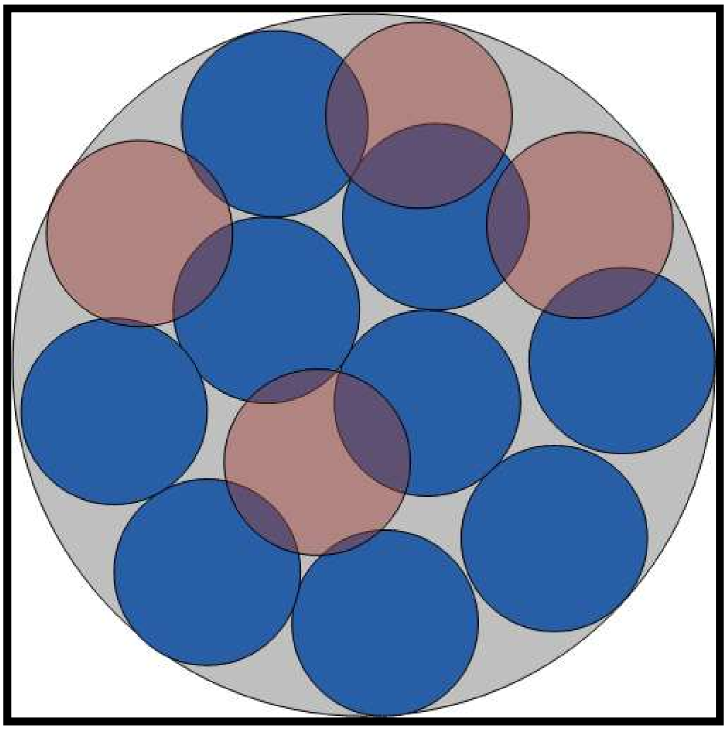

Figure 18: Reducing the effect of free spaces resulting in TDO

Table 4 below provides details of all TDO occurrences within the tower.

Third Degree Overlap		
Occurrence	**Lances**	**Area**
1	1; 25	0.802
2	2; 26	0.436
3	7; 34	0.802
4	8; 35	0.435
5	10; 38	0.240
6	13; 25	0.017
7	13; 26	0.057
8	14; 28	0.017
9	14; 29	0.002
10	15; 31	0.017
11	15; 32	0.017
12	16; 34	0.017
13	16; 35	0.057
14	17, 37	0.017
15	17; 38	0.034
16	18; 40	0.017
17	18; 41	0.017
Total		3.006

Table 4: Table showing occurrence and area (m^2) of TDO

The pie chart below (Figure 19) illustrates the respective percentage of overlap for each overlap classification. The chart clearly and effectively shows that FDO accounts for the vast majority of overlap within the tower. The area of coverage of SDO and TDO are very similar and, when combined, make up just under a quarter of the slurry overlap.

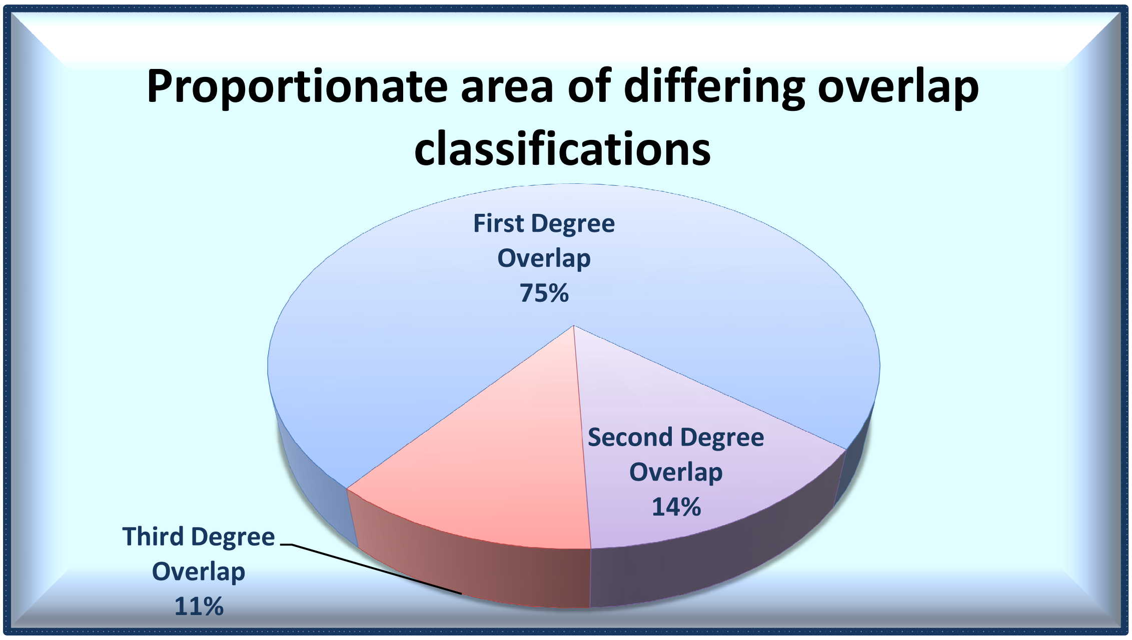

Figure 19: Pie chart illustrating proportions of differing areas of overlap

Figure 20 below graphically shows the number of occurrences of overlap related to each classification. SDO has more than twice the number of occurrences of FDO, and mor than three times the number occurrences of TDO.

By analysing Figures 19 and 20, insight can be gained into the extent of overlap for each classification. When comparing the occurrences and area coverage for each classification, it becomes apparent that, although FDO has fewer occurrences than SDO, the average area of FDO is much greater than that of SDO or TDO. The same could be said for the magnitude of TDO compared with SDO.

The above-mentioned statistics are confirmed by the data in Table 5.

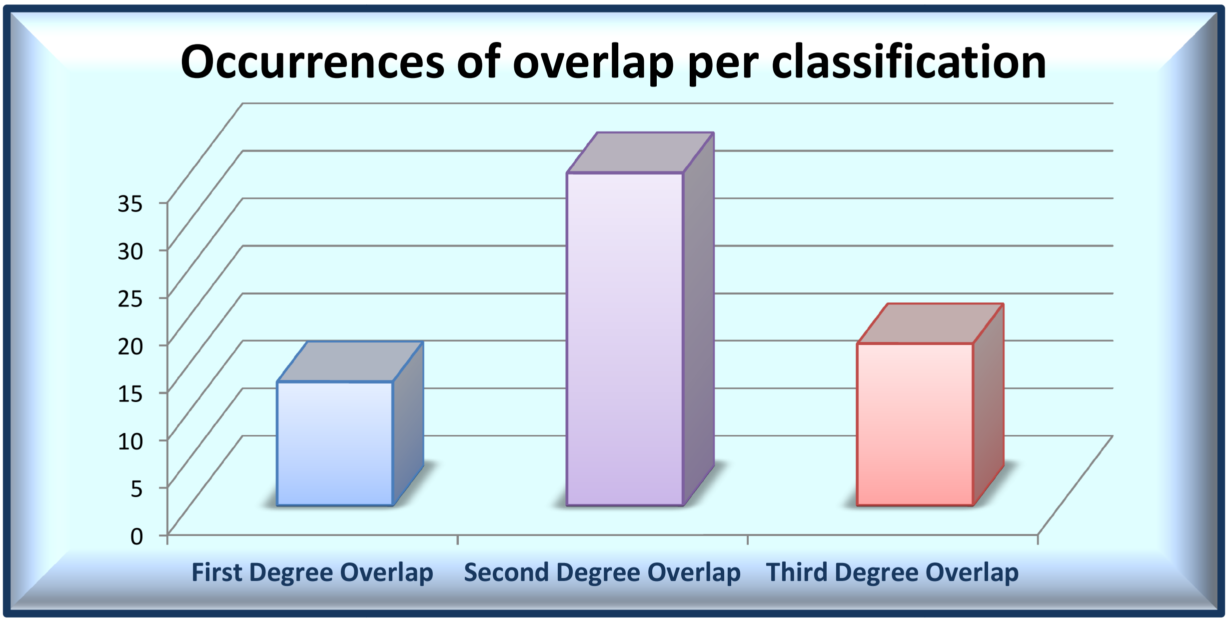

Figure 20: Histogram illustrating occurrences of overlap per classification

The distinction between occurrences and instances is clear when considering Figures 20 and 21. FDO generally has three instances per occurrence, while SDO and TDO always have one instance per occurrence.

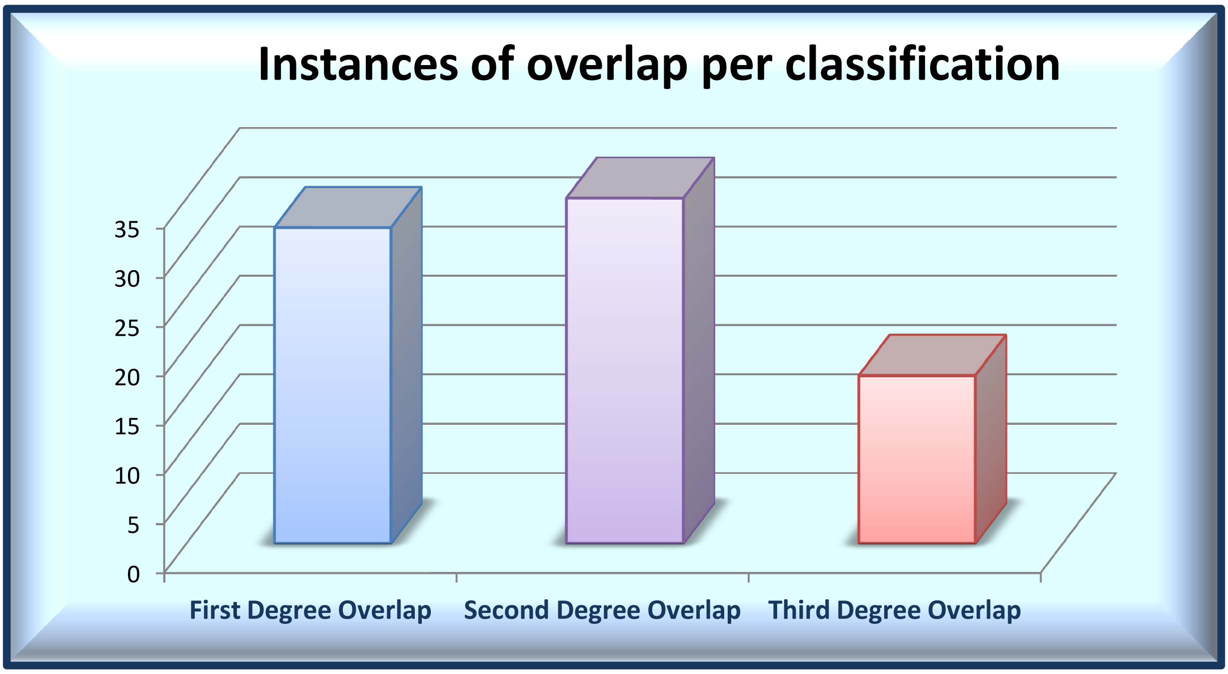

Figure 21: Histogram illustrating the instances of overlap per classification

Classification statistics							
	Average Area	Median	Minimum	Maximum	Area Range	Occurrences	Total Area
FDO	1.497	1.279	0.699	2.701	2.003	13	19.458
SDO	0.102	0.0725	0.0207	0.4761	0.4554	35	3.569
TDO	0.177	0.0171	0.0026	0.8024	0.7997	17	3.006

Table 5: Overlap statistics per classification

Various statistics are relevant to a thorough analysis of the current configuration of lances. These statistics are summarised in the table above. They show clearly that occurrences of FDO are significantly larger than the other two classifications. The difference between the average and the median area values shows that the distributions of overlap measurements are skew. The range provides insight into the differences in the extent of overlap per classification.

A small amount of slurry originating from the bottom layer of lances is sprayed against the side of the tower; but this is not included in the overlap calculations. Figure 22 below illustrates this occurrence. The slurry that makes contact with the inside of the tower tends to 'bounce' off the side, rather than streaming down the side. This is because, by the time the slurry reaches a diameter large enough to make contact with the tower, it has dried enough to be more of a powder than a viscous slurry.

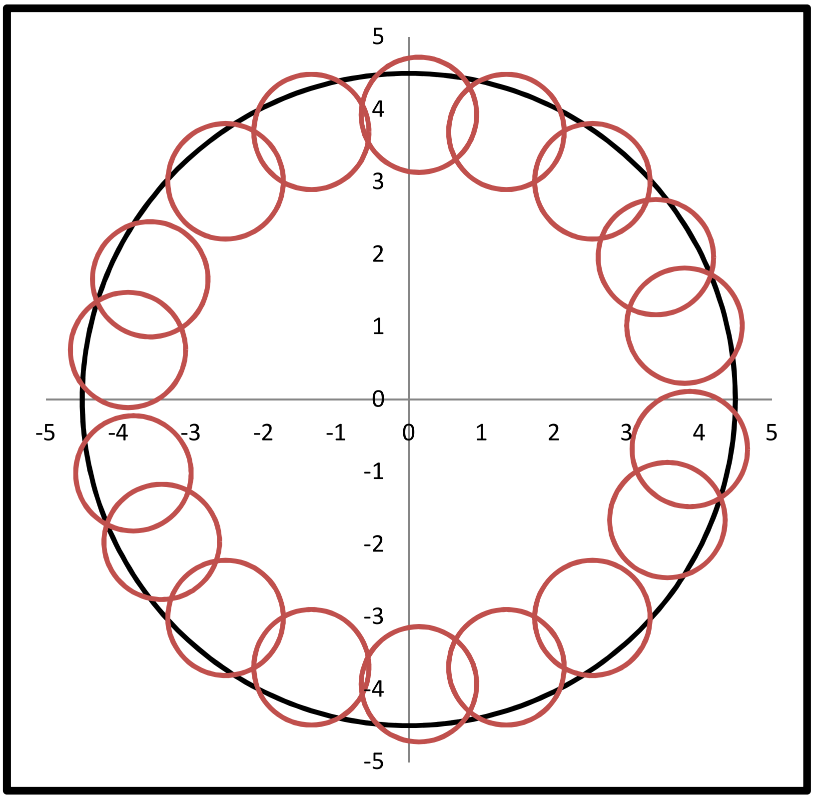

Figure 22: Illustration of slurry originating from the bottom layer of lances making contact with the tower

4.2.2 Open Space Analysis

Using an Excel simulation of the current lance configuration, the position and size of the open spaces within the drying tower are easily identified. These are illustrated in Figure 22, using an edited version of the screen-shot of the Excel simulation. The yellow, green, and purple spaces represent areas of FDS, SDS, and TDO respectively. There is only one instance of FDS, located in the centre of the tower. From Figure 22 below, it is evident that the presence of the FDS has a significant impact on the efficiency of the tower, which ultimately influences the efficiency of the furnace, where more gas is burned to compensate for the loss in energy within the tower. The presence of the FDS is thus unacceptable and should be remedied.

There are six instances of SDS within the tower. These spaces are all located immediately lateral to the slurry circle originating from the longest lances. The size and shape of the SDS are largely similar – a symptom of the highly symmetrical lance configuration. Whenever circles are packed within any container, there will always be open spaces, which are a result of the inherent shape of circles. These spaces are generally small in proportion to the circles being packed, and aer also more-or-less convexly triangular in shape. These small spaces are classified as TDS, and are largely unavoidable because, by altering the position of lances to reduce TDS, a substantial amount of overlap is created. Figure 23 illustrates this situation.

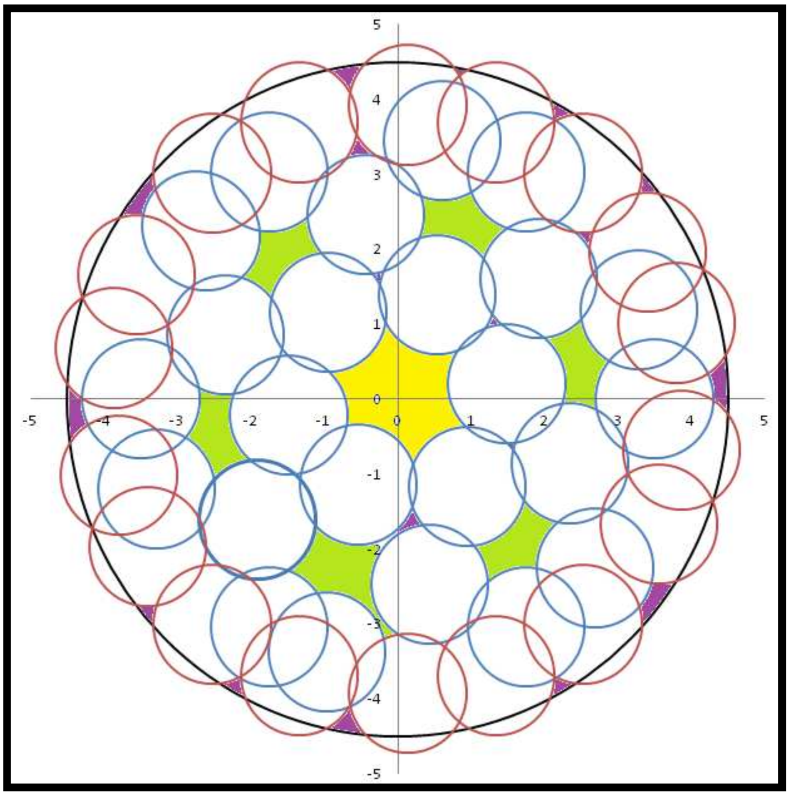

Figure 23: Graphical representation of open spaces in current configuration of lances

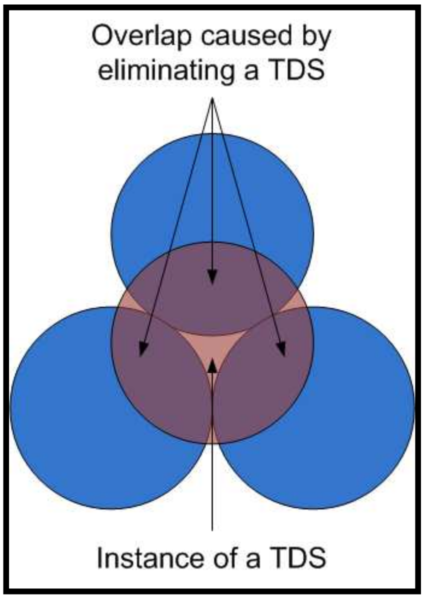

Figure 24: Effect of eliminating a TDS

Figure 24 illustrates the importance of balancing the amount of overlap with the number of open spaces. A solution that minimises both overlap and open space is not feasible when packing circles. The extent of overlap should thus always be a consideration when reducing the free spaces within the system.

Figure 25 below illustrates the number of occurrences for each classification of overlap. From the chart, it is clear that TDS are the most frequent. However, the effect of TDS is minimal, and thus not an important consideration for the analysis of the lance configuration.

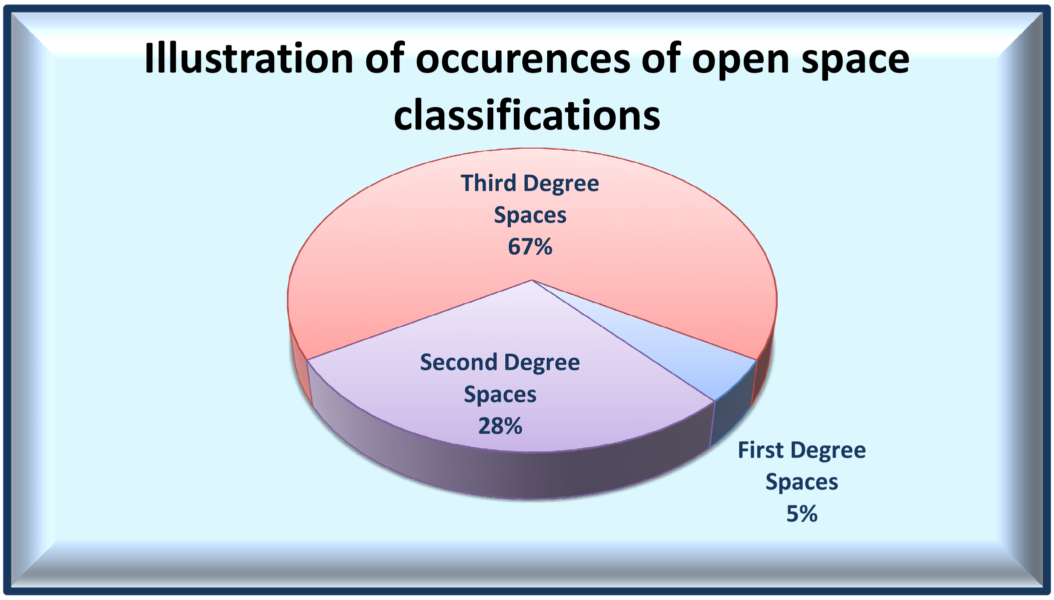

Figure 25: Pie chart illustrating the occurrences of open space classifications

TDS are thus eliminated in the further study of the relationship between the open space classifications. Figure 26 below shows the relationship of occurrences between FDS and SDS.

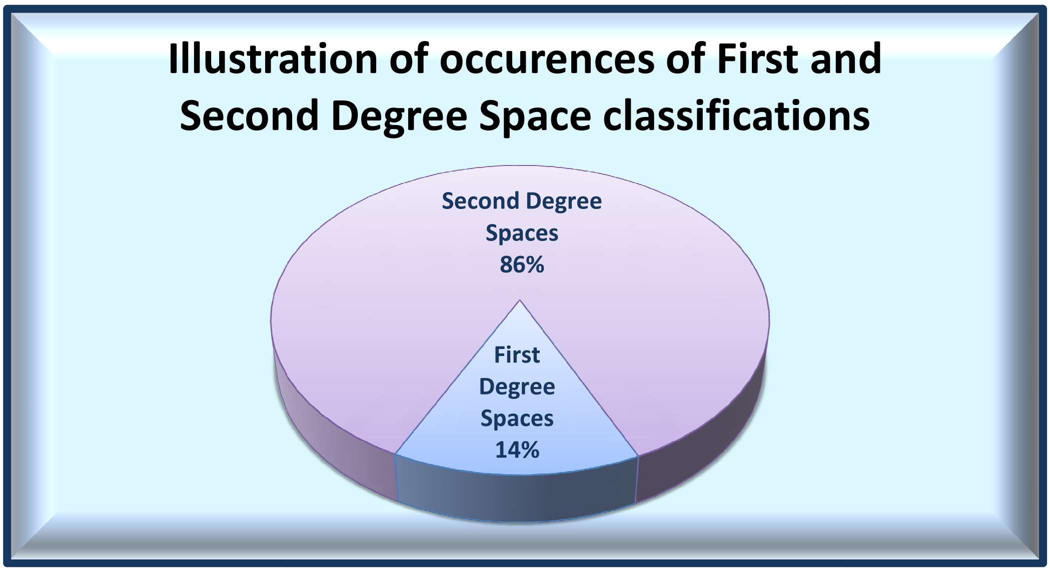

Figure 26: Pie chart illustrating the occurrences of FDS and SDS only

From this diagram, it is clear that there are many more occurrences of SDS than of FDS. The occurrences of SDS should be minimised (and if possible, eradicated), and the single occurrence of FDS should be eliminated. These measures should be taken to avoid the slump in efficiency that is a symptom of the sub-optimal placement of lances.

4.3 Analysis of Proposed Configuration

The proposed solution aims to balance the amount of open space and overlap. This is achieved by optimising the positioning of the top layer of 24 lances. The placement of the bottom layer of lances is then done by positioning the lances in the areas of biggest overlap. It is obvious that a solution without overlap or open spaces is impossible when packing circles into any container; but by using the above-mentioned technique, a very good solution is attained.

Figure 27 below illustrates the proposed configuration to be analysed. The blue and red circles represent the slurry coverage originating from the top and bottom layer of lances respectively. Appendix D illustrates the positioning and numbering of the proposed lance configuration for each layer independently.

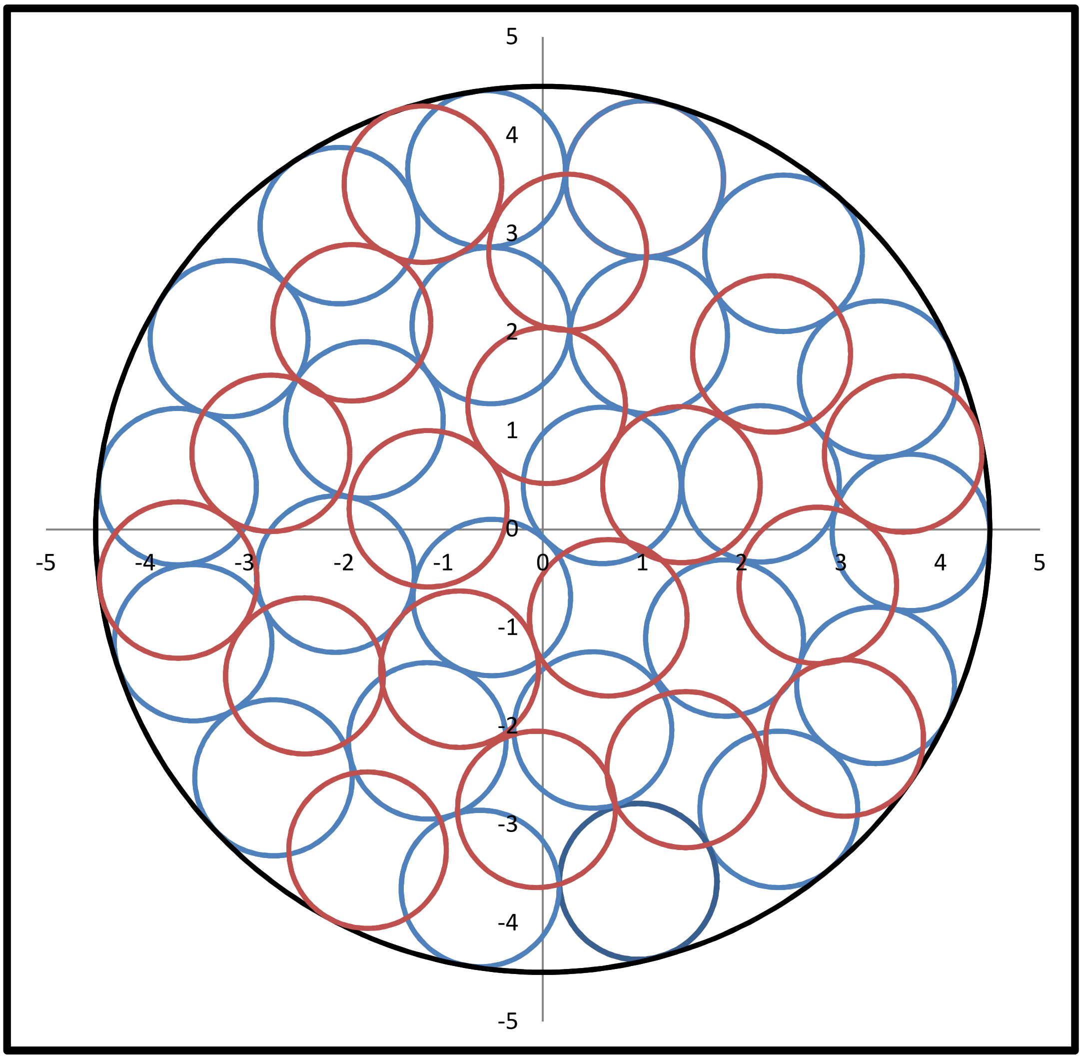

Figure 27: Proposed configuration to be analysed

4.3.1 Overlap Analysis

The calculation of overlap within the proposed solution uses the same method as the analysis of the current configuration overlap, and is based on the rules of trigonometry and geometry explained in Appendix E.

Table 6 below illustrates all the occurrences of overlap within the proposed solution. When examining the proposed configuration, it should be noticed that no intra-layered slurry overlap occurs. The absence of intra-layered overlap means that all overlap within the tower will be classified as TDO. The lack of intra-layered overlap is intentional, and leads to a more even drying of the slurry within the tower. There are 68 instances of overlap (all TDO), with a total of 23.086m^2 of overlapping area.

				TDO				
Occurrence	**Lances**	**Area**	**Occurrence**	**Lances**	**Area**	**Occurrence**	**Lances**	**Area**
1	1; 25	0.276	**21**	12; 32	0.480	**41**	19; 29	0.301
2	1; 26	0.406	**22**	12; 40	0.524	**42**	19; 30	0.301
3	2; 26	0.307	**23**	13; 32	0.242	**43**	19; 35	0.225
4	2; 41	0.964	**24**	13; 33	0.217	**44**	19; 38	0.010
5	3; 27	0.501	**25**	14;25	0.278	**45**	20; 30	0.192
6	3; 41	0.565	**26**	14; 33	0.519	**46**	20; 31	0.295
7	4;27	0.236	**27**	15; 25	0.213	**47**	20; 38	0.765
8	4; 28	0.232	**28**	15; 26	0.095	**48**	20; 42	0.050
9	5; 28	0.508	**29**	15; 33	0.178	**49**	21; 31	0.407
10	5; 39	0.572	**30**	15; 36	0.765	**50**	21; 32	0.102
11	6; 29	0.301	**31**	16; 26	0.406	**51**	21; 37	0.286
12	6; 39	0.572	**32**	16; 27	0.105	**52**	22; 32	0.480
13	7; 29	0.301	**33**	16; 34	0.334	**53**	22; 33	0.519
14	8; 30	0.413	**34**	16; 36	0.001	**54**	22; 37	0.329
15	9; 30	0.301	**35**	17; 27	0.501	**55**	23; 34	0.376
16	9; 42	0.759	**36**	17; 28	0.508	**56**	23; 36	0.765
17	10; 31	0.407	**37**	17; 34	0.376	**57**	23; 37	0.286
18	10; 42	0.758	**38**	18; 28	0.095	**58**	24; 35	0.519
19	11; 31	0.306	**39**	18; 29	0.413	**59**	24; 37	0.137
20	11; 40	0.524	**40**	18; 35	0.519	**60**	24; 38	0.765
				Total				**23.086**

Table 6: Table showing all occurrences of overlap within the proposed configuration

4.3.2 Open Space Analysis

Using an Excel simulation of the positioning of lances and the accompanying slurry overlap, the position and relative size of the open spaces between the circles is easily identified. Figure 28 below shows the positions and sizes of all the open spaces within the tower, indicated in yellow. These spaces are small, and are generally directly adjacent to the container wall. This which makes them largely unavoidable without severely impacting on the amount of overlap within the tower. All the open spaces fall into the TDS classification owing to their size and roughly triangular shape.

Since the positioning of the top layer of lances is optimal and is done before the positioning of the second layer, these positions are fixed. Thus the positioning of the bottom layer of lances has a significant impact on the number and size of open spaces within the configuration. These positions are determined by using maths, and are explained in Appendix D.

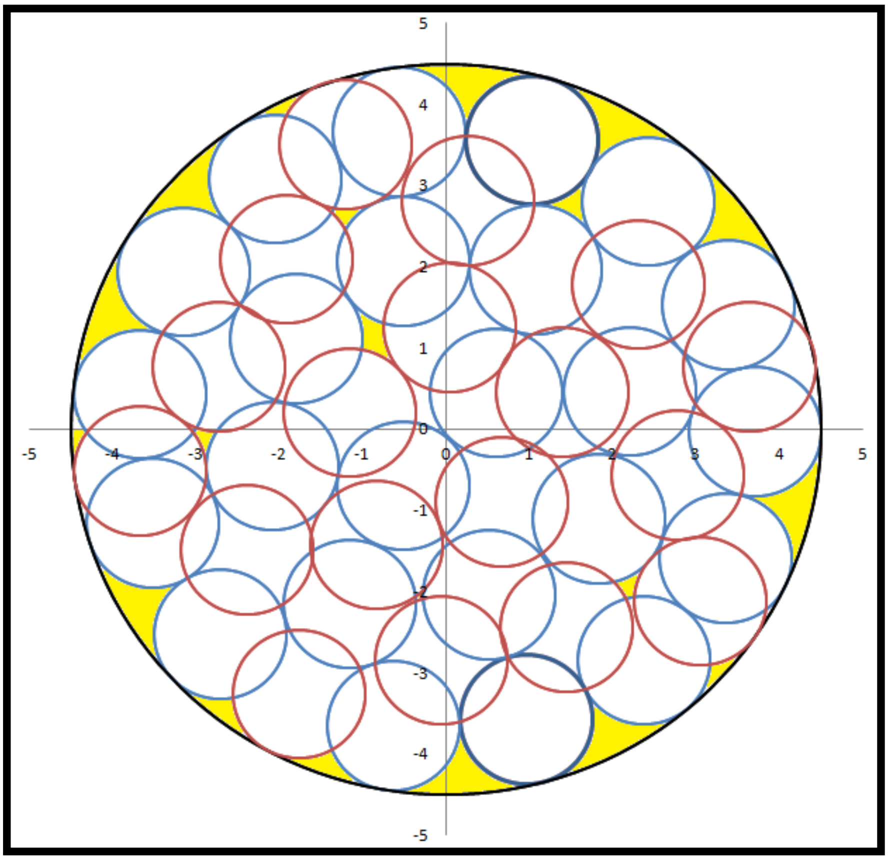

Figure 28: Diagrammatic representation of open spaces in proposed configuration of lances

4.4 Configuration Comparison

When comparing the current and proposed configurations, one must ensure that the radii of the packing circles are equal. An equal radius of packing circles for each configuration indicates that the vertical distances from the lance to the point of measurement are equal. The initial radius of the proposed configuration was 0.0015m (1.5mm) larger than that of the current positioning, which means that the vertical distance is slightly more than for the current configuration. This difference would not have had a significant impact on the measurements. It was decided, however, that the radii should be exactly the same, allowing an unbiased comparison, and that the circles sizes should be equivalent. Thus 3mm was subtracted from the diameter of each circle in the proposed solution.

Figure 29 below shows the positioning of lances and slurry coverage of the top layer of lances for the current and the proposed positioning of lances within the tower. This diagram shows that there is top layer overlap in the current positioning, but not in the proposed positioning. In addition, the proposed positioning of top layered lances has fewer and smaller open spaces than the current positioning. These improvements will have a positive impact on the amount of gas burnt within the furnace to dry slurry to powder.

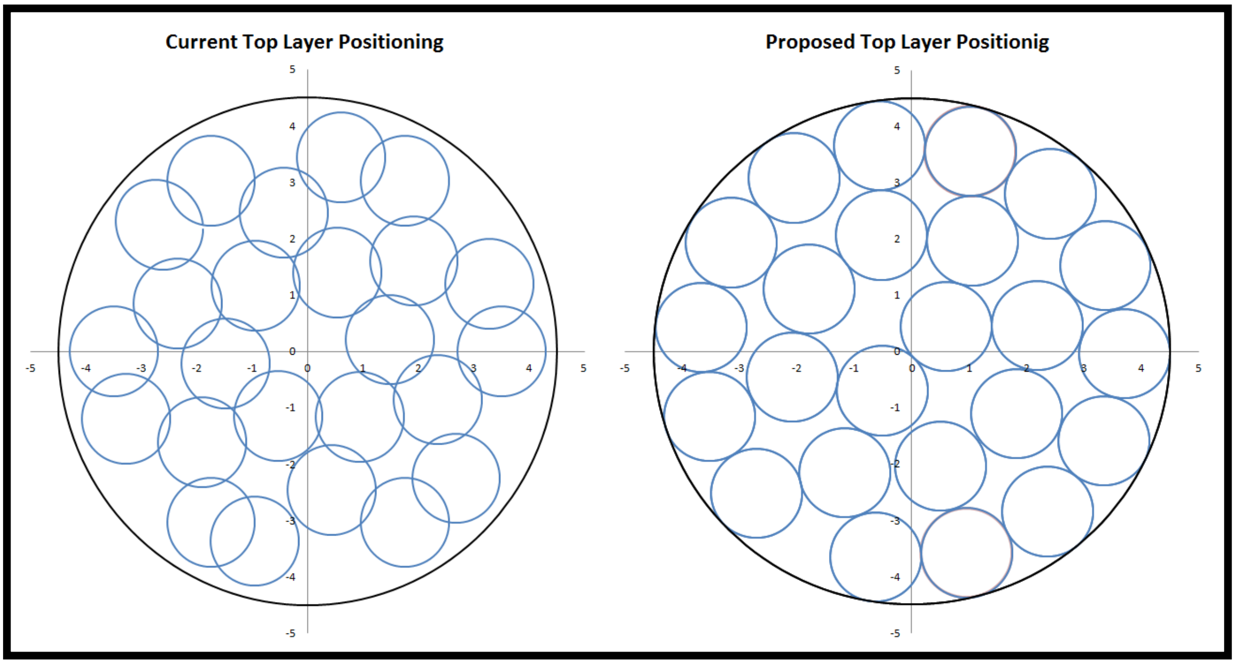

Figure 29: Comparison of top lance layer positioning of current and proposed configurations

Figure 30, shown below, is used to compare the current and the proposed positioning of the bottom layer. The current positioning of the bottom layer of lances causes slurry to strike the side of the tower. This causes a mixture of slurry to 'bounce' off the side of the tower. This leads to an uneven density of slurry, ultimately causing uneven drying. In addition, the current positioning of the bottom layered lances allows an intra-layered overlap of the bottom layer. This overlap negatively impacts on the drying ability of the affected areas of overlap. And the more overlap (especially intra-layered overlap) that occurs, the more will open spaces result from the inefficient use of slurry coverage. The proposed solution, however, does not have any instances of intra-layered overlap. This feature of the proposed configuration makes it possible to deal with, and reduce, the open spaces within the tower.

Figure 31 illustrates the complete configuration for the current and the proposed lance positioning. The current configuration of lances produces 26.033m^2 of overlap, while the proposed solution produces only 23.086m^2 of overlap. The difference is 2.947m^2. This may seem rather small, but, when calculating the area of one slurry circle ($A = \pi r^2 = \pi * 4.5^2$= 1.976m^2), this difference appears more significant. The proposed solution also shows distinctly fewer open spaces than does the current slurry coverage. In effect, by reducing the number of open spaces within the tower, less superheated air will escape through the gaps in the slurry.

In Figure 31, open spaces are highlighted for ease of comparison. From the diagram, one notices that the current positioning has a larger total are of overlap than does the proposed solution. It is also apparent that the majority of the open spaces in the proposed solution are located around the outside of the tower. This would also be the case in the current solution if the slurry originating from the bottom layer of lances were not 'overlapping' with the tower wall.

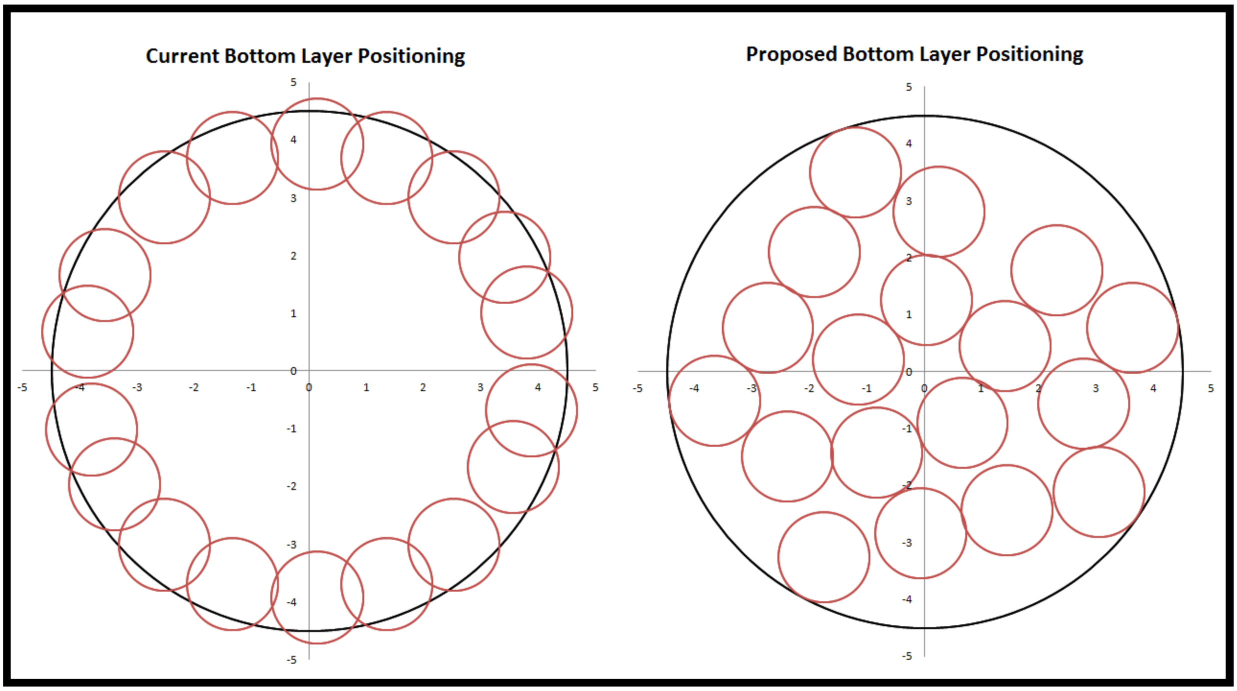

Figure 30: Comparison of bottom lance layer positioning of current and proposed configuration

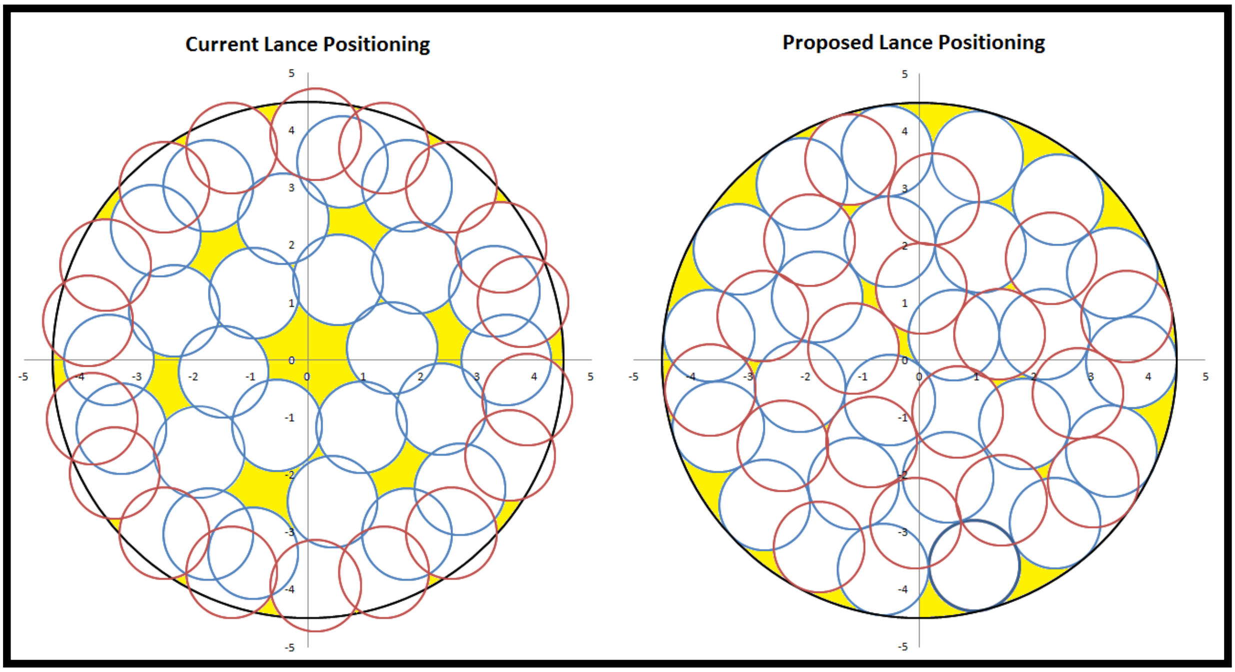

Figure 31: Comparison of lance positioning and slurry coverage of currrent and proposed configuration

The proposed solution provides better slurry coverage than does the current configuration: it reduces both the amount of overlap within the tower and the area of the open spaces within the tower, and it does not spray slurry against the side of the tower.

Because there is no overlap of slurry within the top layer of lances, all lances within the top layer should be opened before any second layer lances are opened. The only factor that should be taken into consideration is the symmetrical opening of lances. Appendix J provides the proposed order in which lances should be opened.

4.5 Results Validation

The results obtained by the models were validated by comparing the results obtained with each program with one another. This comparison confirmed that the initial solution obtained through the use of Lopez and Beasley's FSS algorithm is somewhat flawed. This inaccuracy is most likely the result of an error in the MATLAB coding. However, the solution obtained by the TomSym model showed much more promise, because it provided a solution that seemed to be logically viable. This solution was compared with the 'gold standard' set by the Packomania website. This comparison showed the TomSym solution to be valid. Although the positioning of the circle was not identical, the radius attained from this solution using a polygon with 1,000 sides and 50 different starting positions deviated by less than 0.000001m from the 'gold standard' – a discrepancy that is not problematic in the context of slurry coverage. In addition, the solution could be improved by increasing the number of iterations and sides of the inscribed polygon. The increased accuracy would not be significant, however, and the time needed to run the model would increase significantly. Nevertheless, the origin of the discrepancy should be discussed. When inspecting the solution and lance numbering in Appendix D one notices that two ‘rattlers’ are present. Changing the position of these rattlers changes the solution without affecting its validity.

The validation of results is not only integral to the project, it is also vital to the final decision about future implementation.

Chapter 5

Conclusion

5.1 Recommendations for Implementation

The change management principles described in Chapter 2 should be followed if the project is to be successfully implemented. Thus far, the changes to the configuration of lances have been defined according to the SMART model.

- ***S****pecific:* Specific changes have been proposed to the lance configuration.
- ***M****easurable:* The amount of overlap and number of open spaces for each solution are measured to compare the configurations easily.
- ***A****ctionable:* The people affected by the proposed change should be notified of how and why the change will take place, as well as how the change will affect them.
- ***R****ealistic:* The proposed change is realistic, and has been analysed in depth to ensure this.
- ***T****ime-bound:* The project has been time-bound by completing it within the allotted time frame.

5.2 Conclusion

The proposed solution aims to improve the efficiency of the tower's operations by reducing the amount of gas burnt to convert slurry into base powder within the required PMC. The problem has been solved by applying operations research techniques to solve a variation of the circle packing problem, using Microsoft Excel simulations to gain insight into the current and proposed configurations, and employing mathematical formulae for the placement of bottom layered lances. The aim is achieved by decreasing the amount of slurry overlap and the number of open spaces within the tower. In addition, the operational uniformity of the tower is improved by suggesting the order in which the lances should be opened.

All the results were validated to ensure the correct positioning of the lances. Implementation of the project will reduce the amount of gas that has to be burnt to dry out the slurry. This will drastically reduce the gas expenses and the environmental impact of Unilever Boksburg, which will only be quantified after implementation.

References

[1] C.O. Lopez, J.E. Beasley, A heuristic for the circle packing problem with a variety of containers, *European Journal of Operations Research* 214 (2011: 512-522)

[2] E.G. Birgin, J.M. Gentil, New and improved results for packing of identical unitary radius circles within triangles, rectangles and strips, *Computer & Operations Research* 37 (2008: 2357-2375)

[3] W.D. Kelton, R.P. Sadowski, N. B. Swets, *Simulation with Arena 5th Edition* 2010

[4] R. Skeith, G. Curry, D. Hairston, Simulation checks the problem of machine interface, *Industrial Engineering* (1969: 22-25)

[5] J. Lui, S. Xue, Z. Lui, D. Xu, An improved energy landscape paving algorithm for the problem of packing circles into a larger containing circle, *Computers & Industrial Engineering* 57 (2009: 1144-1149)

[6] J.S. Smith, Survey on the use of simulation for manufacturing system design and operation, *Journal of Manufacturing Systems* 22 (2003: 157-171)

[7] C. Leggett, A case study of a batch manufacturing plant simulation, *European Journal of Operational Research* (1978: 1-7)

[8] K. Cho, I. Moon, W. Yun, System analysis of a multi-product, small-lot-sized production by simulation: a Korean Motor Factory case, *Computers & Industrial Engineering* 30 (1996: 347-357)

[9] J.K. Klitz, Simulation of an automated logistics and manufacturing system, *European Journal of Operational Research* 14 (1989: 36-40)

[10] Open Group, The (2007), The Open Group Architecture Framework (TOGAF) Version 8.1.1, Enterprise Edition.

[11] www.mathworld.wolfram.com/NP-HardProblem.html

[12] A.M. Brown, A methodology for simulating biological systems using Microsoft Excel, *Computer Methods and Programs in Biomedicine* (1997: 181-190)

[13] I. Meineke, J. Brockmöller, Simulation of complex pharmacokinetic models in Microsoft Excel, *Computer Methods and Programs in Biomedicine* (2007: 239-245)

[14] R.J.W. Lambert, I. Mytilinaios, L. Maitland, A.M. Brown, Monte Carlo simulation of parameter confidence intervals for non-linear regression analysis of biological data using Mircosoft Excel, *Computer Methods and Programs in Biomedicine* (2011: 1-9)

[15] www.packomania.com

[16] www.analyzemath .com

[17] www.tomsym.com

[18] www.investopedia.com

Interviews & Discussions

Mrs G.J Botha- Mentor, University of Pretoria Lecturer

Prof Yadavalli Head of Department of Industrial Engineering at the University of Pretoria

Dr A.C. Janse van Rensburg- University of Pretoria Senior Lecturer

Mr O. Ferreira- Head of Maintenance at Unilever Boksburg

Mr J. Conradie- Process and Innovation Engineer at Unilever Household Care and Laundry, Boksburg

Appendix A

Factory Information

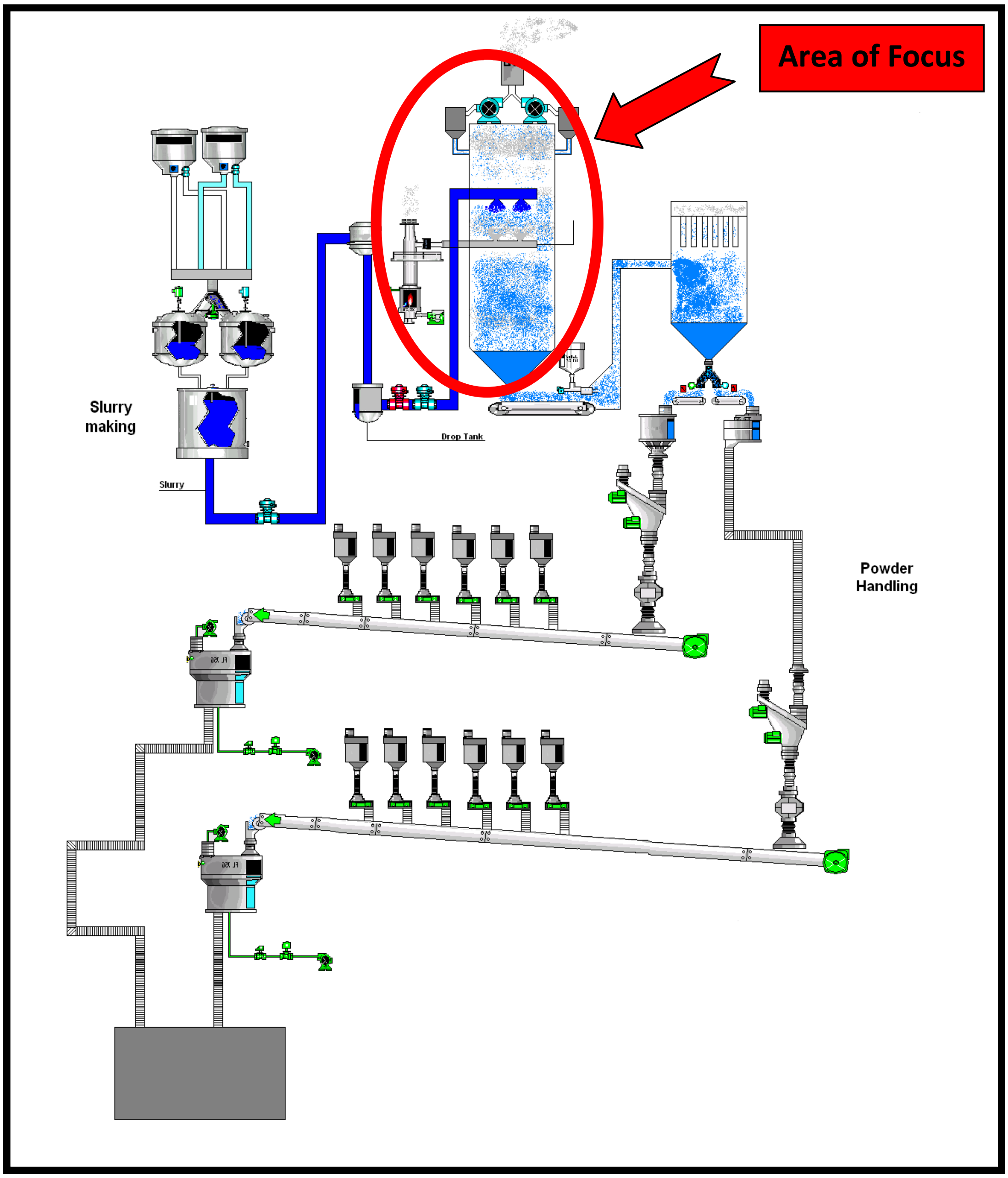

Figure 32: Basic factory layout, Unilever Boksburg

Appendix B

Current oscillation of gas usage

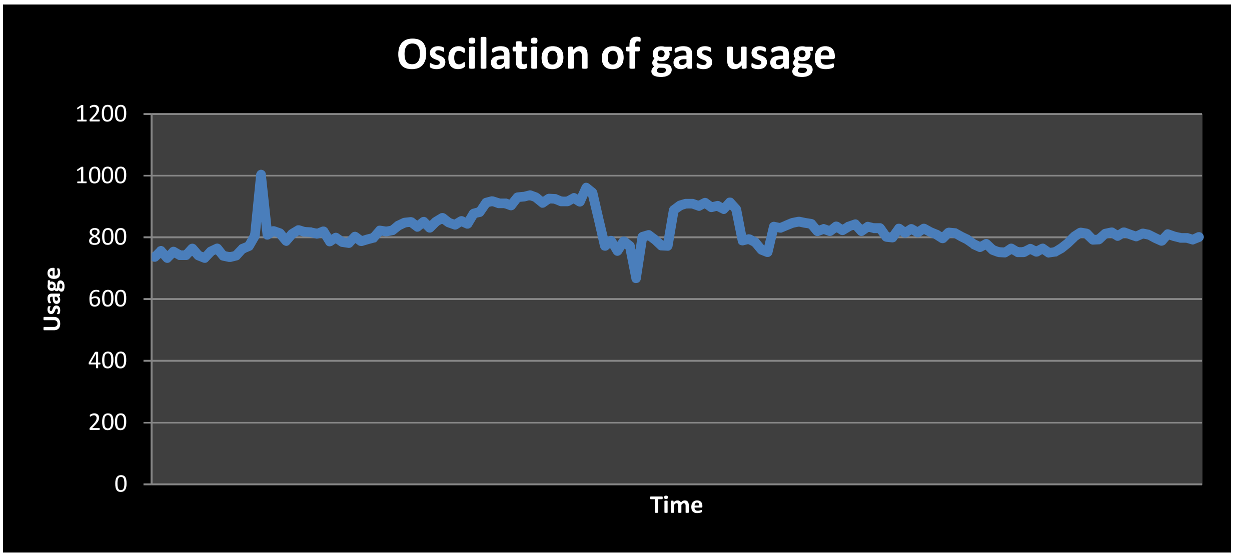

Figure 33: Oscillation of gas usage

Appendix C

Current configuration and lance numbering

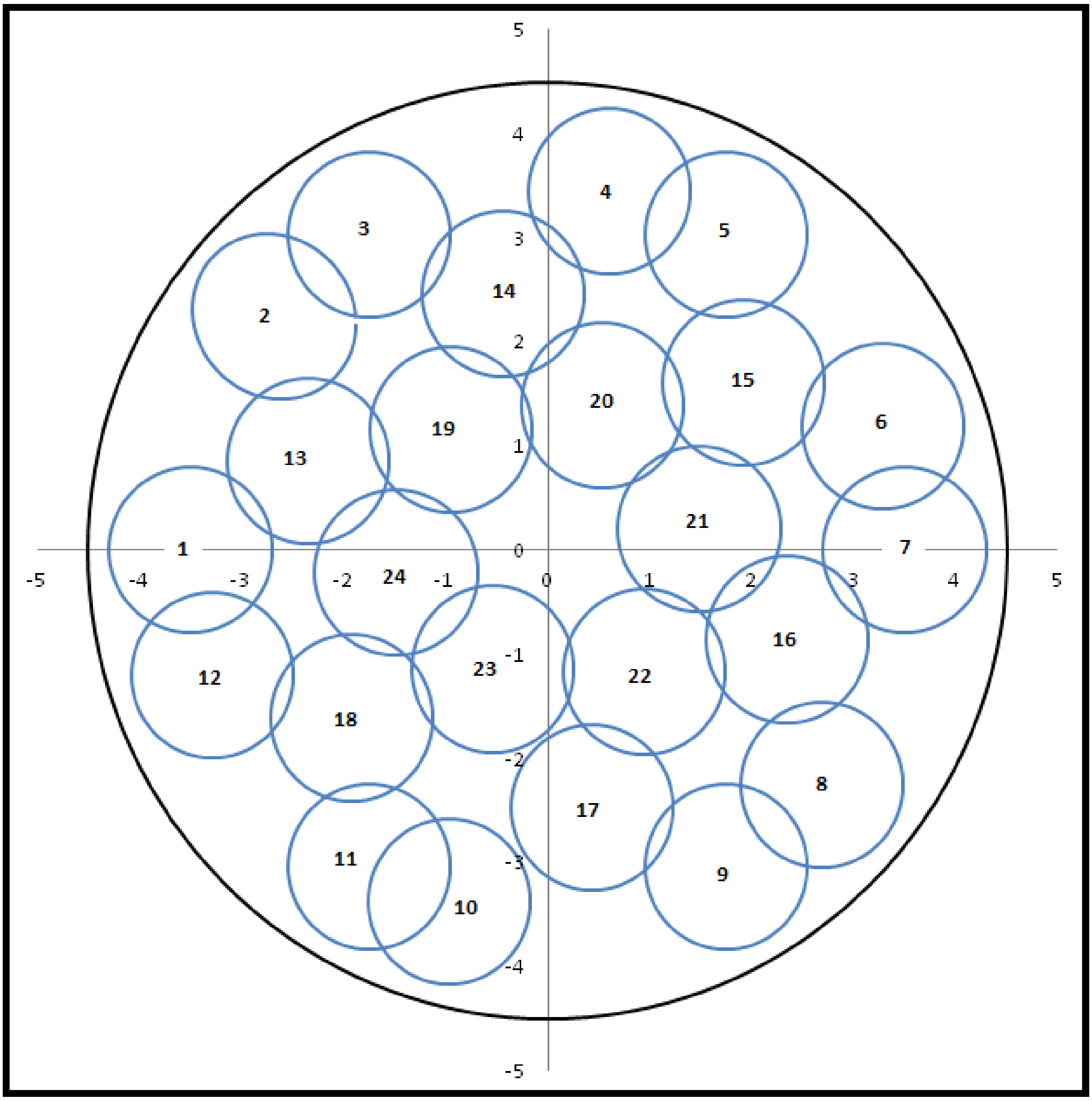

Figure 34: Illustration of top layer lance positioning and numbering with accompanying slurry coverage for current configuration

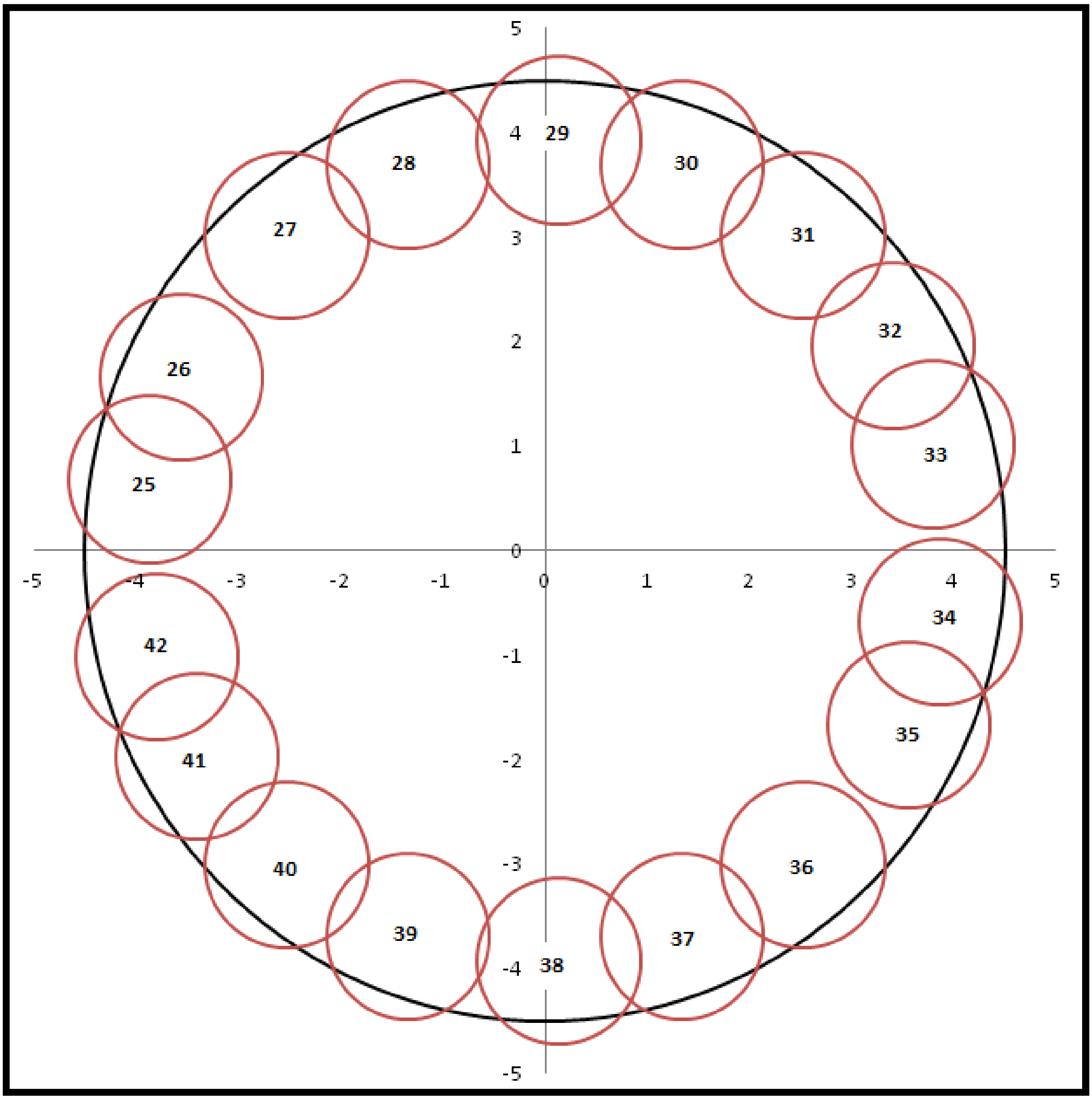

Figure 35: Illustration of bottom layer lance positioning and numbering with accompanying slurry coverage for current configuration

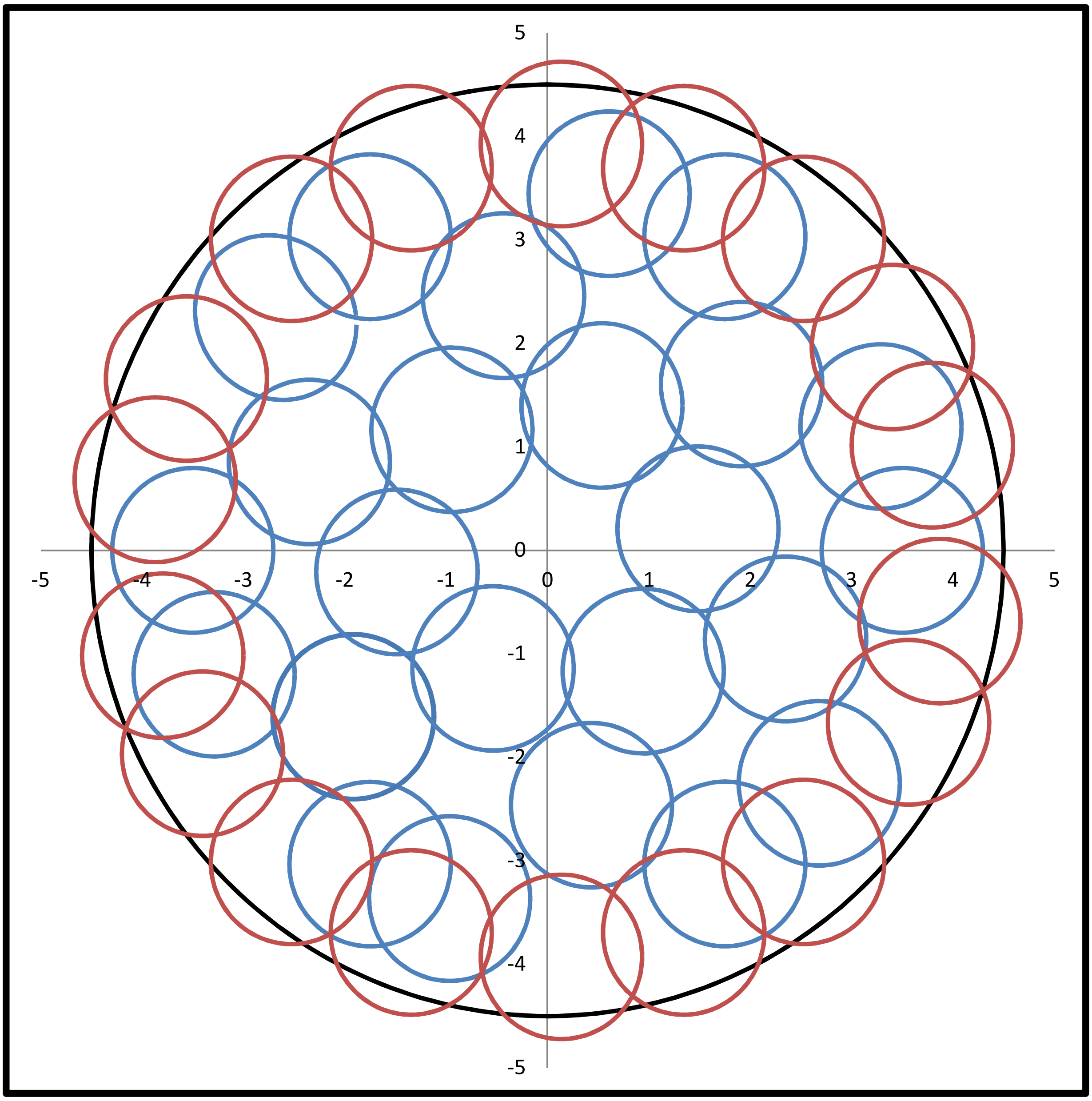

Figure 36: Illustration of top and bottom layer lance positioning with accompanying slurry coverage for current configuration

The lance numbering is not given in Figure 36 for the sake of simplicity.

Appendix D

Calculation of Bottom Lance Layer Positions

Figure 37 below illustrates the solution to the circle packing problem given by the TomSym model. This solution represents the configuration of the top layer of lances for the proposed solution.

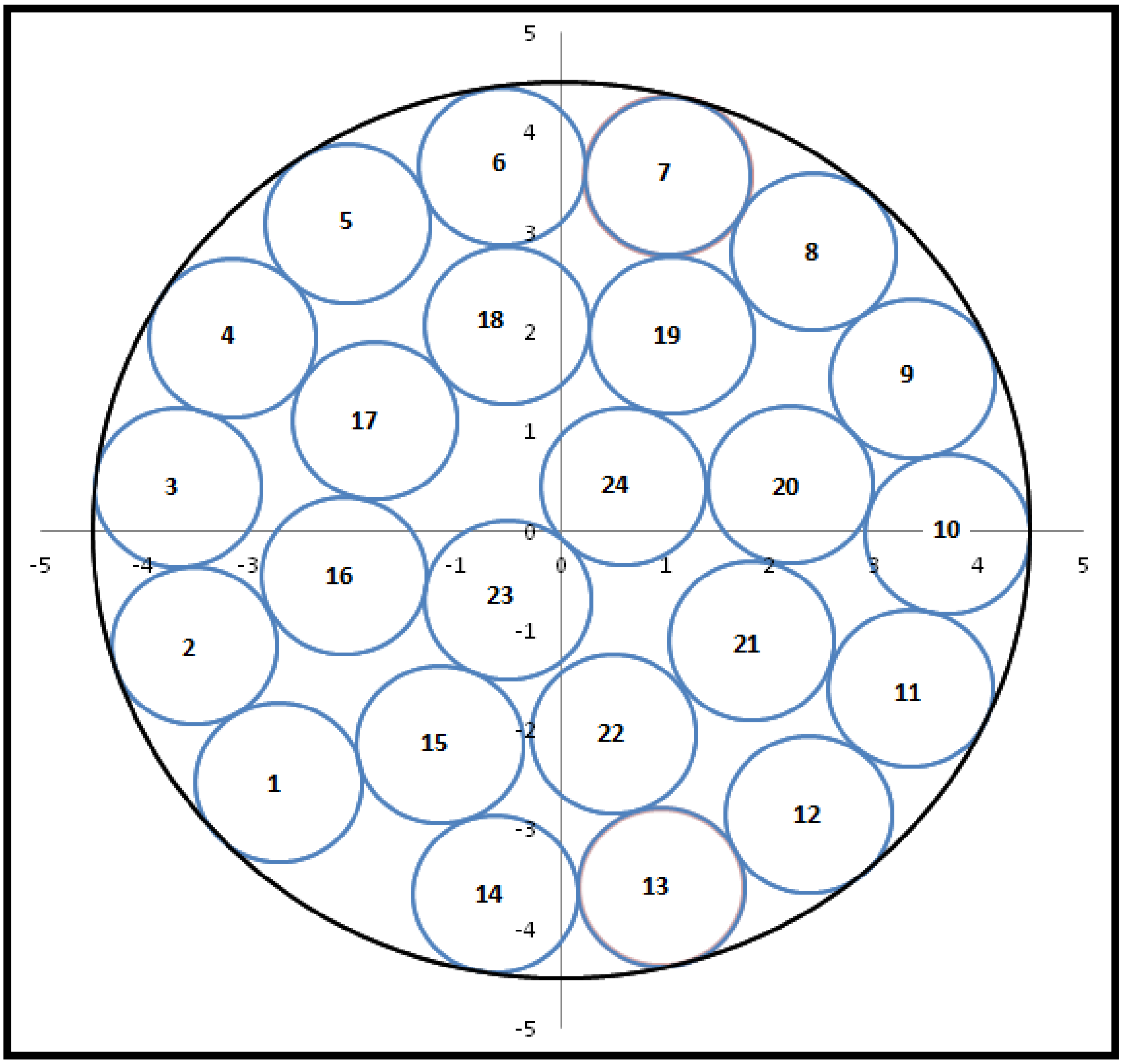

Figure 37: Illustration of lance numbering for the top layer of the proposed solution

Using the above positions of the top layer of lances and the respective slurry coverage, the positions of bottom layer lances can be calculated. The objective of the bottom layer is to maximise the coverage of slurry within the tower while minimising the overlap between lances.

This objective is attained by positioning the second layer of lances in the gaps between the top layer of lances.

The positioning of the bottom layer of lances is calculated using Polar and/or Cartesian coordinates, depending on the positioning of the lance relative to others. Figure 38 below illustrates the positioning of the bottom layer of lances within the proposed configuration.

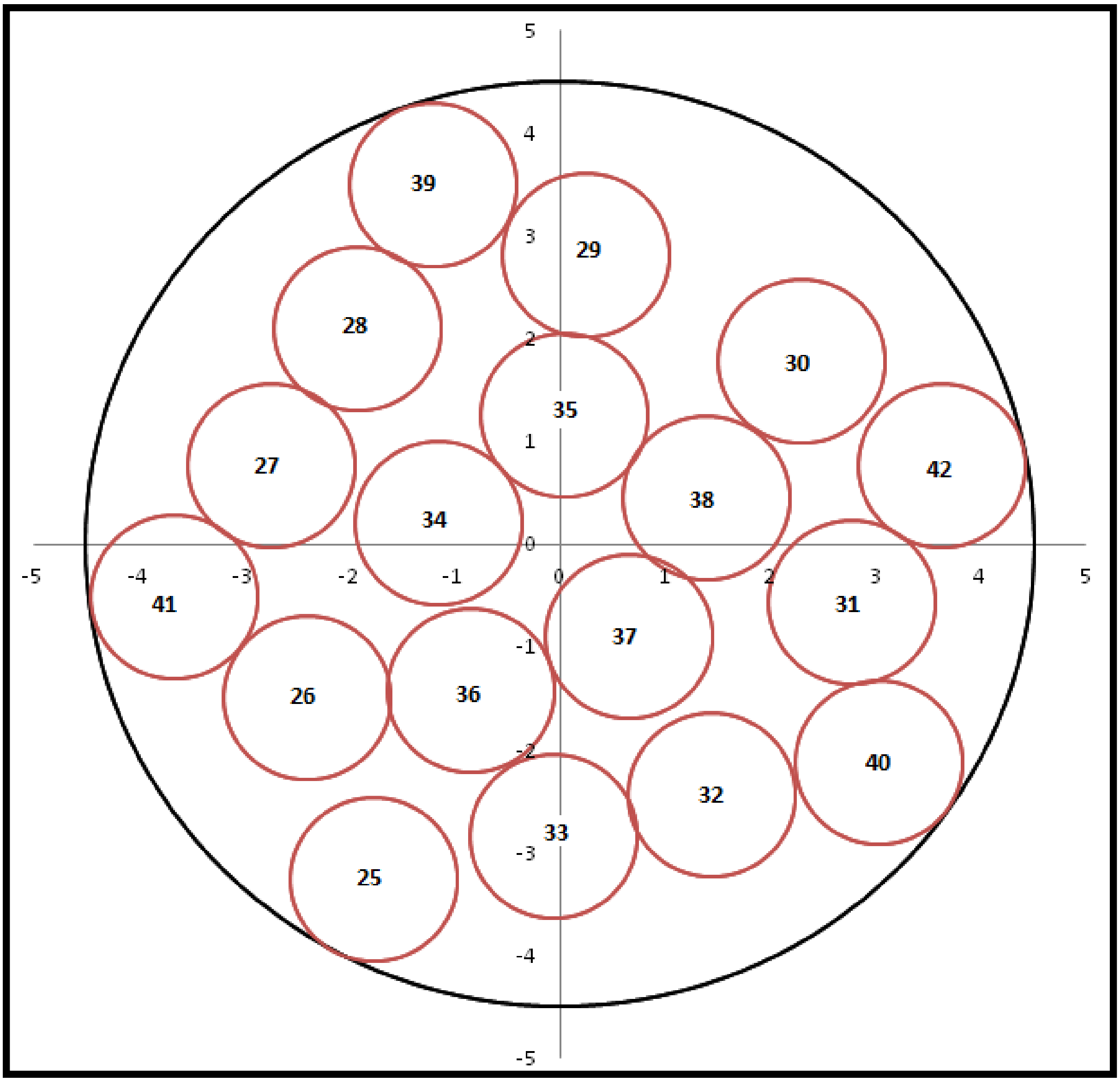

Figure 38: Illustration of final lance positioning with accompanying slurry flow

Description of Second Layer Lance Positioning

The cross sectional slurry area at 1.35m below the lance is used to identify appropriate positioning. Refer to Figures 37 and 38 above to gain understanding into position calculation description of lances 25 to 42.

Lance 25: The Polar coordinate system is used to calculate the angle from the origin to the position of 15. This angle provides the correct line on which the lance should be placed. The length is determined by subtracting the radius of the slurry circle from the radius of the tower, 4.5m.

Lance 26: The placement is attained through calculating the x and y coordinates of the midpoint between lance 1 and 16.

Lance 27: The placement is attained through calculating the x and y coordinates of the midpoint between lance 3 and 17.

Lance 28: The placement is attained through calculating the x and y coordinates of the midpoint between lance 5 and 17.

Lance 29: The placement is attained through calculating the x and y coordinates of the midpoint between lance 7 and 18.

Lance 30: The placement is attained through calculating the x and y coordinates of the midpoint between lance 9 and 19.

Lance 31: The placement is attained through calculating the x and y coordinates of the midpoint between lance 10 and 21.

Lance 32: The placement is attained through calculating the x and y coordinates of the midpoint between lance 12 and 22.

Lance 33: The placement is attained through calculating the x and y coordinates of the midpoint between lance 14 and 22.

Lance 34: The placement is attained through calculating the x and y coordinates of the midpoint between lance 17 and 23.

Lance 35: The placement is attained through calculating the x and y coordinates of the midpoint between lance 18 and 24.

Lance 36: The placement is attained through calculating the x and y coordinates of the midpoint between lance 15 and 23.

Lance 37: The placement is attained through calculating the x and y coordinates of the midpoint between lance 21 and 23.

Lance 38: The placement is attained through calculating the x and y coordinates of the midpoint between lance 20 and 24.

Lance 39: The Polar coordinate system is used to calculate the angles from the origin to the position of lances 5 and 6. The midpoint of these two angles provides the correct line on which the lance should be placed. The length is determined by subtracting the radius of the slurry circle from the radius of the tower, 4.5m.

Lance 40: The Polar coordinate system is used to calculate the angles from the origin to the position of lances 11 and 12. The midpoint of these two angles provides the correct line on which the lance should be placed. The length is determined by subtracting the radius of the slurry circle from the radius of the tower, 4.5m.

Lance 41: The Polar coordinate system is used to calculate the angles from the origin to the position of lances 2 and 3. The midpoint of these two angles provides the correct line on which the lance should be placed. The length is determined by subtracting the radius of the slurry circle from the radius of the tower, 4.5m.

Lance 42: The Polar coordinate system is used to calculate the angles from the origin to the position of lances 9 and 10. The midpoint of these two angles provides the correct line on which the lance should be placed. The length is determined by subtracting the radius of the slurry circle from the radius of the tower, 4.5m.

Appendix E

Calculation of overlapping circles

The calculation of the area of overlapping circles is essential to the comparison of the current and proposed lance positioning. The method of solution is obtained from www.analysemath.com and from www.mathforum.org.

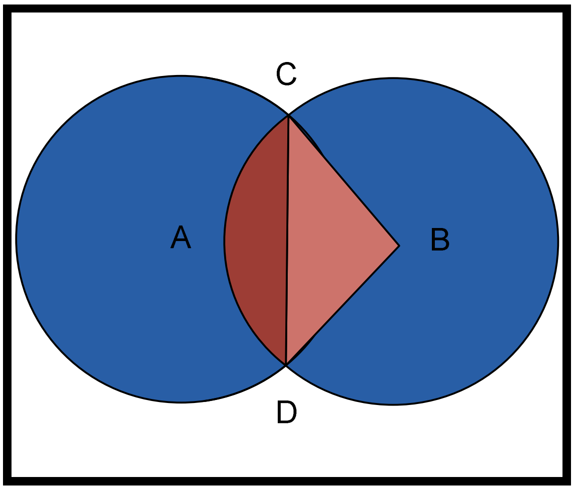

Figure 39: Overlapping circles calculation demonstration circles

Because all circles are identical, the overlap can be split exactly into halves. Thus, by obtaining the solution for one half, this value can be multiplied by two to provide the solution. The solution is obtained as follows:

Let A and B be the centre of circles one and two respectively.

- Calculate distance between A and B.
  AB = $\sqrt{(X\ Axis\ Distance)^2 + (Y\ Distance)^2}$
- Calculation of area
  $r_1^2 = r_2^2 + AB^2 - 2(r_2)(AB)\cos(CBA)$
  $\cos(CBA) = (r_2^2 + AB^2 - r_1^2)/ 2(r_2)(AB)$
  Thus: CBD = 2CBA
  CAD = CBD (equal circle sizes)
  Express angles in ***radians***

AREA = $2\,((0.5(CBD)\,r_2^2\,) - (0.5(r_2^2(\mathrm{Sin}(CBD)))$

The area calculation subtracts triangle CBD from the segment CBD, thus giving the area of half the overlap. This value is then doubled to give the entire area of overlap.

Table of current positions of slurry circles			
Circle	**X-coordinate**	**Y-coordinate**	**Radius**
1	-3.5	0	0.7951
2	-2.681155508	2.249756685	0.7951
3	-1.749999913	3.031088964	0.7951
4	0.607768638	3.446827133	0.7951
5	1.750000044	3.031088888	0.7951
6	3.288924213	1.197070391	0.7951
7	3.5	0	0.7951
8	2.681155508	-2.25	0.7951
9	1.749999913	-3.03	0.7951
10	-0.964730771	-3.364415928	0.7951
11	-1.750000044	-3.031088888	0.7951
12	-3.288924213	-1.197070391	0.7951
13	-2.349231544	0.855050381	0.7951
14	-0.43412035	2.462019399	0.7951
15	1.915111146	1.606968978	0.7951
16	2.349231544	-0.855050381	0.7951
17	0.43412035	-2.462019399	0.7951
18	-1.915111146	-1.606968978	0.7951
19	-0.943980558	1.165718965	0.7951
20	0.537551938	1.400370634	0.7951
21	1.485402111	0.208759593	0.7951
22	0.943980558	-1.165718965	0.7951
23	-0.537551938	-1.140037063	0.7951
24	1.485402111	-0.208759593	0.7951
25	-3.870294466	0.682437357	0.7951
26	-3.561789583	1.660889811	0.7951
27	-2.526155234	3.010554722	0.7951
28	-1.344139039	3.692992045	0.7951
29	0.137154856	3.927605956	0.7951
30	1.344139039	3.692992045	0.7951
31	2.526155234	3.010554722	0.7951
32	3.403479809	1.965000049	0.7951
33	3.79608849	1.017158875	0.7951
34	3.870294466	-0.682437357	0.7951
35	3.561789583	-1.660889811	0.7951
36	2.526155234	-3.010554722	0.7951
37	1.344139039	-3.692992045	0.7951
38	0.137154856	-3.927605956	0.7951
39	-1.344139039	-3.692992045	0.7951
40	-2.526155234	-3.010554722	0.7951
41	-3.403479809	-1.965000049	0.7951
42	-3.79608849	-1.017158875	0.7951

Table 7: Cartesian coordinates of cross-sectional slurry flow of current lance positioning

Using the coordinates, the distances between midpoints were calculated. There are 42 circles in total. The reduced table below shows only the distances between the first eight circles.

Reduced table of distances								
	1	**2**	**3**	**4**	**5**	**6**	**7**	**8**
1	0.0000	2.3941	3.5000	5.3623	6.0622	6.8937	7.0000	6.5779
2	2.3941	0.0000	1.2155	3.5000	4.4995	6.0622	6.5778	7.0002
3	3.5000	1.2155	0.0000	2.3941	3.5000	5.3623	6.0622	6.8938
4	5.3623	3.5000	2.3941	0.0000	1.2155	3.5000	4.4995	6.0624
5	6.0622	4.4995	3.5000	1.2155	0.0000	2.3941	3.5000	5.3626
6	6.8937	6.0622	5.3623	3.5000	2.3941	0.0000	1.2155	3.5002
7	7.0000	6.5778	6.0622	4.4995	3.5000	1.2155	0.0000	2.3944
8	6.8843	7.5261	7.5090	6.8016	6.1333	4.2716	3.1397	0.0000

Table 8: Reduced table of distances between circle centres

The radius calculation for cross-sectional circles was performed using simple trigonometry mathematics. Refer to the calculations and to Figure 20 below.

The measurement of the cross-section is taken at 1.35 metres below the lance; thus:

Measurement taken at 1.35m
a = b = 1.35/sin(59.5)
a = b =1.5668m

Cosine rule
$c^2 = a^2 + b^2 - 2ab*Cos(\vartheta)$

c = $\sqrt{(1.5668)^2 + (1.5668)^2 - 2(1.5668)(1.5668)Cos(61)}$
c = 1.59042m (diameter)
The radius of circle is thus = 0.7951

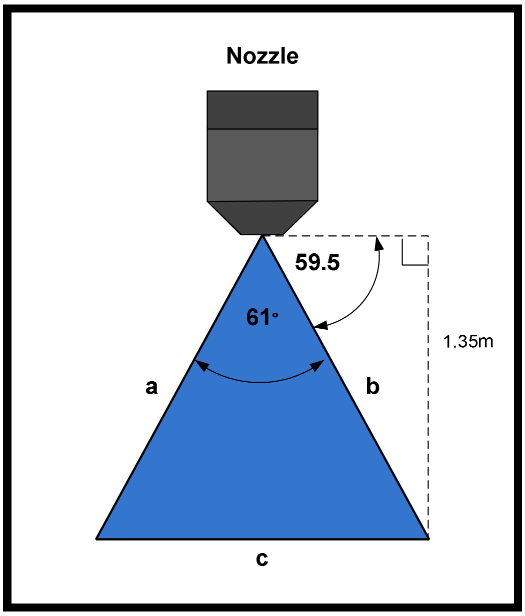

Figure 40: Calculation of diameter of circle

If the distance between centres is more than two times the radius, 1.5904m, there will be no overlap; however, if this distance is less than 1.5904m, there will be overlap. The smaller the measured distance between circles centres, the more overlap will occur between the circles. This is illustrated in Table 9 below. Owing to the format of the table, duplicates do occur refer to Tables 9 and 10 below – because the table treats circle 'A' overlapping with 'B' as a separate and different occurrence than circle 'B' overlapping with circle 'A'.

Reduced table of distances								
	1	**2**	**3**	**4**	**5**	**6**	**7**	**8**
1	0.0000	N/A	N/A	N/A	N/A	N/A	N/A	N/A
2	N/A	0.0000	1.2155	N/A	N/A	N/A	N/A	N/A
3	N/A	1.2155	0.0000	N/A	N/A	N/A	N/A	N/A
4	N/A	N/A	N/A	0.0000	1.2155	N/A	N/A	N/A
5	N/A	N/A	N/A	1.2155	0.0000	N/A	N/A	N/A
6	N/A	N/A	N/A	N/A	N/A	0.0000	1.2155	N/A
7	N/A	N/A	N/A	N/A	N/A	1.2155	0.0000	N/A
8	N/A	N/A	N/A	N/A	N/A	N/A	N/A	0.0000

Table 9: Reduced table of distances between overlapping circles

Further Modified Table of Overlapping Distances								
	1	2	3	4	5	6	7	8
1	0	N/A	N/A	N/A	N/A	N/A	N/A	N/A
2	N/A	0	1.215537	N/A	N/A	N/A	N/A	N/A
3	N/A	1.215537	0	N/A	N/A	N/A	N/A	N/A
4	N/A	N/A	N/A	0	1.215537	N/A	N/A	N/A
5	N/A	N/A	N/A	1.215537	0	N/A	N/A	N/A
6	N/A	N/A	N/A	N/A	N/A	0	1.215537	N/A
7	N/A	N/A	N/A	N/A	N/A	1.215537	0	N/A
8	N/A	N/A	N/A	N/A	N/A	N/A	N/A	0

Table 10: Further modified table of distances between circle centres

Using the method and formulae explained previously, with the data from the current lance positioning, Table 11 below was produced to illustrate the amount of overlap between certain lances. Note that only the bottom left half of the table is used, to avoid a duplication of results. Additionally, the "overlap" between the same lance (e.g. 1 and 1) is not considered as overlap because obviously the area of calculated area of overlap is equal to the area of the circle. These values are highlighted in red in Table 11 below.

Reduced table showing area of Overlap								
Area	**1**	**2**	**3**	**4**	**5**	**6**	**7**	**8**
1	1.986	0	0	0	0	0	0	0
2	0	1.986	0.263	0	0	0	0	0
3	0	0.263	1.986	0	0	0	0	0
4	0	0	0	1.986	0.263	0	0	0
5	0	0	0	0.263	1.986	0	0	0
6	0	0	0	0	0	1.986	0.263	0
7	0	0	0	0	0	0.263	1.986	0
8	0	0	0	0	0	0	0	1.986

Table 11: Reduced table of overlapping areas between circles

Appendix F

Converting the solution from a unit circle container to the appropriate nine metre diameter

The solution is initially given in the form of Cartesian coordinates. Table 12 below illustrates the initial positioning of the circles within a unit circle.

Containing unit circle: Cartesian coordinates			
	X (m)	Y (m)	Radius
1	-0.456	0.685	0.177
2	-0.702	0.430	0.177
3	0.750	0.339	0.177
4	-0.602	-0.561	0.177
5	0.527	-0.632	0.177
6	0.227	0.791	0.177
7	0.538	0.623	0.177
8	0.133	0.099	0.177
9	0.112	-0.453	0.177
10	-0.464	-0.101	0.177
11	-0.399	0.247	0.177
12	0.487	0.103	0.177
13	0.823	-0.007	0.177
14	-0.140	-0.811	0.177
15	-0.259	-0.477	0.177
16	-0.782	-0.256	0.177
17	0.406	-0.246	0.177
18	-0.817	0.096	0.177
19	-0.114	-0.154	0.177
20	-0.126	0.813	0.177
21	0.237	0.437	0.177
22	0.744	-0.352	0.177
23	0.213	-0.795	0.177
24	-0.116	0.460	0.177

Table 12: The Cartesian coordinates and radii of contained circles within a unit circle container

Once the solution for the unit circle is obtained, it has to be altered to apply to a containing circle with a nine metre diameter. This alteration is performed by multiplying the radius and the x and y coordinates by a factor of 4.5. The result of this process is illustrated in Table 13 below.

Containing circle with radius of 4.5m: Cartesian coordinates			
	X (m)	Y (m)	Radius
1	-2.711	-2.524	0.7938
2	-3.520	-1.152	0.7938
3	-3.678	0.433	0.7938
4	-3.157	1.937	0.7938
5	-2.052	3.084	0.7938
6	-0.567	3.660	0.7938
7	1.022	3.560	0.7938
8	2.422	2.802	0.7938
9	3.375	1.526	0.7938
10	3.704	-0.033	0.7938
11	3.348	-1.585	0.7938
12	2.373	-2.844	0.7938
13	0.959	-3.577	0.7938
14	-0.632	-3.650	0.7938
15	-1.163	-2.148	0.7938
16	-2.088	-0.455	0.7938
17	-1.796	1.110	0.7938
18	-0.524	2.068	0.7938
19	1.066	1.968	0.7938
20	2.190	0.462	0.7938
21	1.829	-1.105	0.7938
22	0.504	-2.038	0.7938
23	-0.514	-0.694	0.7938
24	0.598	0.446	0.7938

Table 13: Table showing the Cartesian coordinates and radii of contained circles within a 4.5m radius circular container

Using the above positions for the configuration of the lances, the slurry coverage can be illustrated by using graphing software such as MATLAB.

Appendix G

MATLAB coding: Formulation Space Search

The MATLAB coding below is my interpretation of Lopez and Beasley's (2011) FSS model, described in their *European Journal of Operations Research* article, 'A heuristic for the circle packing problem with a variety of containers'.

```
Initialisation: Use Packomania “Gold Standard” as the initial solution.

%OverlapSet returns set of circes that may ovelap
function Q = OverlapSet(circles, delta, R_overlap)
Q = 0;
for n  = 1:length(circles)
    circ1 = circles(n,:);
    for m = n+1:length(circles)
        circ2 = circles(m,:);

        x1 = circ1(1);
        x2 = circ2(1);

        y1 = circ1(2);
        y2 = circ2(2);

        Xov1 = (x1-delta) - (x2 + delta);
        Xov2 = (x1+delta) - (x2-delta);

        Xmin = 0;
        if Xov1 < 0 || Xov2 < 0
            Xvect = [((x1-delta)-(x2-delta))^2 ((x1-delta)-(x2+delta))^2
                ((x1+delta)-(x2-delta))^2 ((x1+delta)-(x2+delta))^2];
            Xmin = min(Xvect);
        end

        Yov1 = (y1-delta) - (y2 + delta);
        Yov2 = (y1+delta)-(y2-delta);

        Ymin = 0;
        if Yov1 < 0 || Yov2 < 0
            Yvect = [((y1-delta)-(y2-delta))^2 ((y1-delta)-(y2+delta))^2
                ((y1+delta)-(y2-delta))^2 ((y1+delta)-(y2+delta))^2];
            Ymin = min(Yvect);
        end

        Mag = Xmin + Ymin;

        if Mag < 4*R_overlap^2
            if Q(1,1)==0;
                Q = [n m];
            else
                Q = [Q; n m];
            end
```

```
        end
    end
end


%Solve NLP
function NEWCirCPos = SolveNLP(X0Y0, C, P,  Q, XY, delta, Roverlap)

N = length(XY); %Number of Circles
toms r; % Radius of Circles

c = tom('c',length(C),2) %Cartesian Circles
p = tom('p',length(P),2) %PolarCircles
clear pi;

Ci = 0;
for i=1:1:length(C)
    if i==1
        Ci = [X0Y0(C(i), 1) X0Y0(C(i), 2)];
    else
        Ci = [Ci; X0Y0(C(i), 1) X0Y0(C(i), 2)];
    end
end

Pi = 0;
for i=1:1:length(P)
    X = X0Y0(i, 1);
    Y = X0Y0(i, 2);

    rad = sqrt(X^2 + Y^2);
    theta = acos(X/rad);

    if Y < 0
        theta = 2*pi - theta;
    end

    if i==1
        Pi = [rad theta];
    else
        Pi = [Pi; rad theta];
    end
end

%Constraints
C2 = cell(length(Ci), 1);
for i =1:1:length(Ci)
    C2{i} = c(i,1)^2 + c(i,2) <= (1-r)^2;
end

C3 = cell(length(Pi), 1);
for i =1:1:length(Pi)
    C3{i} = p(i,1) <= 1-r;
end
```

```
Cart = 0;
for i=1:1:length(Q)
    x = Q(i, 1);
    xi = find(C==x);
    y = Q(i, 2);
    yi = find(C==y);

    if ismember(x, C) && ismember(y, C)
        if Cart(1,1) ==0
            Cart = [xi yi];
        else
            Cart = [Cart; xi yi];
        end
    end
end


C4 = cell(length(Cart), 1);
for i =1:1:length(Cart)
    C4{i} = (c(Cart(i,1),1)-c(Cart(i,2),1))^2 + (c(Cart(i,1),2)-
c(Cart(i,2),2))^2 >= 4*r^2;
end

Pol = 0;
for i=1:1:length(Q)
    x = Q(i, 1);
    xi = find(P==x);
    y = Q(i, 2);
    yi = find(P==y);

    if ismember(x, P) && ismember(y, P)
        if Pol(1,1) ==0
            Pol = [xi yi];
        else
            Pol = [Pol; xi yi];
        end
    end
end

C5 = cell(length(Pol), 1);
for i =1:1:length(Pol)
    C5{i} = p(Pol(i,1),1)^2 + p(Pol(i,2),1)^2-
2*p(Pol(i,2),1)*p(Pol(i,1),1)*cos(p(Pol(i,1),2)-p(Pol(i,2),2)) >= 4*r^2;
end

CP = 0;
for i=1:1:length(Q)
    x = Q(i, 1);
    xi = find(C==x);
    y = Q(i, 2);
    yi = find(P==y);
    if ismember(x, C) && ismember(y, P)
        if CP(1,1) ==0
            CP = [xi yi];
        else
```

```
                CP = [CP; xi yi];
            end
        end

        xi = find(P==x);
        yi = find(C==y);
        if ismember(x, P) && ismember(y, C)
            if CP(1,1) ==0
                CP = [yi xi];
            else
                CP = [CP; yi xi];
            end
        end
end

C6 = cell(length(CP), 1);
for i =1:1:length(CP)
    Const = (c(CP(i,1),1) - p(CP(i,2),1)*cos(p(CP(i,2),2)))^2 + (c(CP(i,1),2)
- p(CP(i,2),1)*sin(p(CP(i,2),2)))^2;
    C6{i} = Const >= 4*r^2;
end

C7 = cell(2*length(Ci), 1);
for i =1:1:length(Ci)
    C7{2*i-1} = -1 <= c(i,1);
    C7{2*i} = c(i,1) <= 1;
end

C8 = cell(2*length(Ci), 1);
for i =1:1:length(Ci)
    C8{2*i-1} = -1 <= c(i,2);
    C8{2*i} = c(i,2) <= 1;
end

C9 = cell(2*length(Pi), 1);
for i =1:1:length(Pi)
    C9{2*i-1} = 0 <= p(i,1);
    C9{2*i} = p(i,1) <= 1;
end

C10 = cell(2*length(Pi), 1);
for i =1:1:length(Pi)
    C10{2*i-1} = 0 <= p(i,2);
    C10{2*i} = p(i,2) <= 2*pi;
end

C11 = {0 <= r, r <= Roverlap};

Co = zeros(length(C), 2);
for i = 1:1:length(C)
    Co(i, 1) = XY(C(i),1);
end
Po = zeros(length(P), 2);
for i = 1:1:length(P)
    Po(i, 1) = XY(P(i),1);
```

```
end
Po = CartToPol(Po);

C16a = cell(2*length(Ci), 1);
for i =1:1:length(Ci)
    C16a{2*i-1} = Co(i,1)-delta <= c(i,1);
    C16a{2*i} = c(i,1) <= Co(i,1)+delta;
end

C16b = cell(2*length(Ci), 1);
for i =1:1:length(Ci)
    C16b{2*i-1} = Co(i,2)-delta <= c(i,2);
    C16b{2*i} = c(i,2) <= Co(i,2)+delta;
end

C16c = cell(2*length(Pi), 1);
for i =1:1:length(Pi)
    C16c{2*i-1} = sin(Po(i,2))*Po(i,1)-delta <= sin(p(i,2))*p(i,1);
    C16c{2*i} = sin(p(i,2))*p(i,1) <= sin(Po(i,2))*Po(i,1)+delta;
end

C16d = cell(2*length(Pi), 1);
for i =1:1:length(Pi)
    C16d{2*i-1} = cos(Po(i,2))*Po(i,1)-delta <= cos(p(i,2))*p(i,1);
    C16d{2*i} = cos(p(i,2))*p(i,1) <= cos(Po(i,2))*Po(i,1)+delta;
end


Constraints = {C2, C3, C4, C5, C6, C7, C8, C9, C10, C11, C16a, C16b, C16c,
C16d};

x0 = {c == Ci, p == Pi};

options = struct;
options.solver= 'multimin';
options.xInit = 5;
solution = ezsolve(-r, Constraints, x0, options);

Ci = solution.c;
Pi = solution.p;

for i=1:1:length(Ci)
    XY(C(i),1) = Ci(i, 1);
    XY(C(i),2) = Ci(i, 2);
end

Pi = PolToCart(Pi);
for i=1:1:length(Pi)
    XY(P(i),1) = Pi(i, 1);
    XY(P(i),2) = Pi(i, 2);
end

NEWCirCPos = XY;
```

```
end
%Correct Radius after SNOPT has run

function Rs = CorrectRadius(X0Y0, XY)

for i=1:1:length(XY)
    if (XY(i,1)^2 + XY(i,2)^2) > 1
        if (X0Y0(i,1)^2 +X0Y0(i, 2)^2) >1
            Pol = CartToPol(XY);
            r = rand(1,1);
            theta = Pol(i,2);
            x = r*cos(theta);
            y = r*sin(theta);
            XY(i,1) = x;
            XY(i,2) = y;
        else
            XY(i,1) = X0Y0(i, 1);
            XY(i,2) = X0Y0(i, 2);
        end
    end
end

Rtemps = 0;
for i=1:1:length(XY)
    x_i = XY(i,1);
    y_i = XY(i,2);
    for j = i+1:1:length(XY)
        x_j = XY(j,1);
        y_j = XY(j,2);

        rad = sqrt((x_i-x_j)^2+(y_i-y_j)^2)/2;

        if Rtemps == 0
            Rtemps = rad;
        else
            Rtemps = [Rtemps rad];
        end
    end
end

R = min(Rtemps);

temp = 0;
for i=1:1:length(XY)
    t = 1 - sqrt(XY(i,1)^2 + XY(i,2)^2);

    if temp == 0
        temp = t;
    else
        temp = [temp t];
    end
end

Rs = min([R min(temp)]);
```

```
%Change the Polar and Cartesian coordinates of circles
function p = PolToCart(RT)

p =0;

for i =1:1:length(RT)
    r = RT(i, 1);
    theta = RT(i,2);

    x = r*cos(theta);
    y = r*sin(theta);

    if p(1,1) == 0
        p = [x y];
    else
        p = [p; x y];
    end
end
return
```

Appendix H

MATLAB coding: TomSym

The code below was obtained from the TomSym website (www.tomsym.com). This coding was developed by TomSym, and is available in the model library as an example of a circle packing problem within an inscribed polygon. The green text describes the meaning of the corresponding line of code.

```
N = 1500;    % Represents the Number of sides of the inscribed polygon. The
             larger this number, the more accurate the solution. This occurs
             because the polygon starts resembling the shape of a circle
M = 24;      % Number of circles to fit within the inscribed polygon

toms r                   % Radius of the packing circles
x = tom('x', 2, M);      % X and Y coordinates of the packing circle centers

clear pi     % Clearing pi gives the variable pi its mathematically correct
             value of 3.1415...

theta = 2*pi/N;          % Theta represents the angle covered by each side of
                         the polygon. Thus, the more sides the polygon has (N)
                         the smaller the value of theta

cdist = cos(theta/2);    % cdist represents the distance from the origin to
                         the midpoint of the sides of the polygon

% The following equations create a set of equations that state that all
circles have to be inside the polygon
phi = theta*(0:N-1)'; % Direction of the normal to the side of the polygon
polyEq = ( [cos(phi) sin(phi)]*x <= cdist-r );

% The following equations create a set of equations that state that no
circles may overlap
circEq = cell(M-1,1);
for i=1:M-1
    circEq{i} = ( sqrt(sum((x(:,i+1:end)-repmat(x(:,i),1,M-i)).^2)) >= 2*r );
end

% Starting guess produces an Initial Solution
x0 = { r == 0.5*sqrt(1/M), x == 0.3*randn(size(x)) };

% Solve the problem, maximizing r
options = struct;
% Try multiple starting guesses and choose best result
options.solver = 'multimin';
options.xInit = 100; % Number of different starting guesses
solution = ezsolve(-r,{polyEq,circEq},x0,options);

% Plot the result
```

```
plot(cos(phi([1:end 1])+theta/2),sin(phi([1:end 1])+theta/2),'-') % Polygon
axis image
hold on
alpha = linspace(0,2*pi,100);
cx = solution.r*cos(alpha);
cy = solution.r*sin(alpha);
for i=1:M
    plot(solution.x(1,i)+cx,solution.x(2,i)+cy) % Circle number i
end
hold off
title(['Maximum radius = ' num2str(solution.r)]);
```

Appendix I

Coordinates of solution

The table below provides the Cartesian coordinates of the final positioning of both top and bottom layered lances.

	X (m)	Y (m)	Radius
1	-2.711	-2.524	0.7938
2	-3.520	-1.152	0.7938
3	-3.678	0.433	0.7938
4	-3.157	1.937	0.7938
5	-2.052	3.084	0.7938
6	-0.567	3.660	0.7938
7	1.022	3.560	0.7938
8	2.422	2.802	0.7938
9	3.375	1.526	0.7938
10	3.704	-0.033	0.7938
11	3.348	-1.585	0.7938
12	2.373	-2.844	0.7938
13	0.959	-3.577	0.7938
14	-0.632	-3.650	0.7938
15	-1.163	-2.148	0.7938
16	-2.088	-0.455	0.7938
17	-1.796	1.110	0.7938
18	-0.524	2.068	0.7938
19	1.066	1.968	0.7938
20	2.190	0.462	0.7938
21	1.829	-1.105	0.7938
22	0.504	-2.038	0.7938
23	-0.514	-0.694	0.7938
24	0.598	0.446	0.7938
25	-1.764	-3.259	0.7938
26	-2.400	-1.489	0.7938
27	-2.737	0.771	0.7938
28	-1.924	2.097	0.7938
29	0.249	2.814	0.7938
30	2.220	1.747	0.7938
31	2.766	-0.569	0.7938
32	1.438	-2.441	0.7938
33	-0.064	-2.844	0.7938
34	-1.155	0.208	0.7938

35	0.037	1.257	0.7938
36	-0.839	-1.421	0.7938
37	0.658	-0.900	0.7938
38	1.394	0.454	0.7938
39	-1.207	3.504	0.7938
40	3.036	-2.121	0.7938
41	-3.671	-0.516	0.7938
42	3.626	0.765	0.7938

Appendix J

Proposed Lance Order of Opening

This section provides an excellent order for lances to be opened to keep overlap and spaces to a minimum.

All lances in the top layer should be opened paying attention only to the symmetrical pattern of opening. It should be remembered that at least 15 lances should be open at any given time. The proposed initial 15 lances are lances 1 to 15, the following lances in order are; 19, 17, 21, 16, 20, 22, 18, 23, 24. These lances are chosen to keep the pattern as symmetrical as possible. Following the opening of all top layer lances, bottom layered lances should be opened. These should be opened in an order such that open spaces and overlapping area is minimised. The proposed order is as follows; 25, 34, 37, 30, 29, 28, 31, 32, 35, 26, 33, 27 the remaining lances namely 36, 38, 39, 40, 41 and 42 all cover TDS and produce a similar amount of overlap. Very rarely will the tower operate with over 36 lances. The only consideration for the opening of these lances will be symmetry. Thus, for the sake of completeness, the proposed order is; 41, 42, 39, 36 and lastly lance 38.